

Change Points in Affine Term-Structure Models: Pricing, Estimation and Forecasting*

SIDDHARTHA CHIB[†]

KYU HO KANG[‡]

(Washington University in St. Louis)

April 2009, October 2009

Abstract

In this paper we theoretically and empirically examine structural changes in a dynamic term-structure model of zero-coupon bond yields. To do this, we develop a new arbitrage-free one latent and two macro-economics factor affine model to price default-free bonds when all model parameters are subject to change at unknown time points. The bonds in our set-up can be priced straightforwardly once the change point model is formulated in the manner of Chib (1998) as a specific unidirectional Markov process. We consider five versions of our general model - with 0, 1, 2, 3 and 4 change points - to a collection of 16 yields measured quarterly over the period 1972:I to 2007:IV. Our empirical approach to inference is fully Bayesian with priors set up to reflect the assumption of a positive term-premium. The use of Bayesian techniques is particularly relevant because the models are high-dimensional and non-linear, and because it is more straightforward to compare our different change point models from the Bayesian perspective. Our estimation results indicate that the model with 3 change points is most supported by the data and that the breaks occurred in 1980:II, 1985:IV and 1995:II. These dates correspond (in turn) to the time of a change in monetary policy, the onset of what is termed the great moderation, and the start of technology driven period of economic growth. We also utilize the Bayesian framework to derive the

*We thank Taeyoung Doh, Ed Greenberg, Wolfgang Lemke, Hong Liu, James Morley, Srikanth Ramamurthy, Myung Hwan Seo, Yongs Shin, Guofu Zhou, the participants of the 2009 Econometric Society summer meeting, the 2009 Seminar on Bayesian Inference in Econometrics and Statistics, and the 2009 Midwest Econometrics Group meeting, and the referees and the Associate editor of this journal, for their thoughtful and useful comments on the paper. Kang acknowledges support from the Center for Research in Economics and Strategy at the Olin Business School, Washington University in St. Louis.

[†]*Address for correspondence:* Olin Business School, Washington University in St. Louis, Campus Box 1133, 1 Bookings Drive, St. Louis, MO 63130. E-mail: chib@wustl.edu.

[‡]*Address for correspondence:* Department of Economics, Washington University in St. Louis, Campus Box 1208, 1 Bookings Drive, St. Louis, MO 63130. E-mail: khkang@wustl.edu.

out-of-sample predictive densities of the term-structure. We find that the forecasting performance of the 3 change point model is substantially better than that of the other models we examine. (JEL G12, C11, E43)

1 Introduction

In this paper we theoretically and empirically examine structural changes in a dynamic term-structure model of zero-coupon bond yields. We do our analysis in the setting of arbitrage-free multi-factor affine models of the type developed in Duffie and Kan (1996) and Dai and Singleton (2000) though we allow for both latent and macro-economic factors along the lines of Ang and Piazzesi (2003), Ang, Dong, and Piazzesi (2007) and Chib and Ergashev (2009). We depart from the existing modeling of structural changes, however, by relying on a change point process rather than the Markov switching process of Dai, Singleton, and Yang (2007), Bansal and Zhou (2002), and Ang, Bekaert, and Wei (2008).

The model we develop and estimate provides a new perspective on the dynamics of zero-coupon bond prices and yields. One reason is because our change-point approach reflects a different view of regime-changes. In a change point specification, a regime once occupied and vacated is never visited again. In contrast, in a Markov switching model, the regimes recur, which implies that a regime occupied in the past (whether distant or near) can occur in the future. The latter assumption may not be germane if one believes that the confluence of conditions that determine a regime are unique and not repeated.

Another reason is because we derive bond prices under the assumption that all parameters in the model can change whereas in previous work some parameters are assumed to be constant across regimes. Thus, in our formulation, we do not have to decide which parameters are constant and which break. As we show, bond prices can be obtained straightforwardly once the change point process is formulated in the manner of Chib (1998) as a specific unidirectional Markov process.

A third reason is because in our empirical analysis we deal with a larger set of maturities than in previous work. This allows us to get finer view of the term-structure than is possible with a smaller set of maturities. In particular, we apply our model to 16 yields of US T-bills measured quarterly between 1972:I and 2007:IV. An added benefit

of working with these many yields is that (in comparison with models with fewer yields) the model with 16 yields produces the best forecasts of the term-structure. The reason for this, which apparently has not been documented or exploited before, is that the addition of new yields introduces only the parameters that represent the pricing error variances, but because the parameters are subject to several cross-equation restrictions, the additional outcomes are helpful in estimation and, hence, in predictive inferences.

A notable aspect of our approach is that the prior distribution is motivated by economic considerations. In particular, our prior on the parameters reflects the assumption of a positive term-premium, following Chib and Ergashev (2009). Another aspect is that our estimation approach which is implemented by tuned Markov chain Monte Carlo methods, is both feasible and reliable. We apply this approach successfully to fit a model that has 209 parameters. Models of this size in this context would be difficult to fit by non-Bayesian methods because of the severe non-linearities and the potential multi-modality of the likelihood function. Our Bayesian approach is also relevant in this context because it offers a straightforward way to compare different change point models through marginal likelihoods and Bayes factors.

Our empirical analysis is organized around 5 different versions of the general model. These models, which we label as \mathcal{M}_0 , \mathcal{M}_1 , \mathcal{M}_2 , \mathcal{M}_3 and \mathcal{M}_4 , contain 0, 1, 2, 3 and 4 change-points, respectively. Our main findings are as follows. The 3 change point model, \mathcal{M}_3 , is the one that is most supported by the data (in comparison with models with 0, 1, 2 and 4 change-points) and that the breaks occurred in 1980:II, 1985:IV and 1995:II. These change-points can be attributed, in turn, to changes in monetary policy, the onset of what is termed the great moderation, and the start of the technology driven period of economic growth. Thus, the most recent break occurs in 1995, not 1985, as is commonly believed. That the underlying distribution of the term-structure is different in the regimes isolated by these change-points can be seen in Figure 1 where we display the 5%, 50% and 95% quantiles of the yield curve data categorized by regime. As we discuss below, the model estimation reveals that the parameters across regimes are substantially different, which provides support to our approach of letting all the parameters vary across regimes. We find, for instance, that the mean-reversion parameters in the factor dynamics and the factor loadings are regime-specific. We conclude our empirical analysis

by predicting the yield curve out-of-sample and find that the predictive performance of our best model is substantially better than that of the other models we consider.

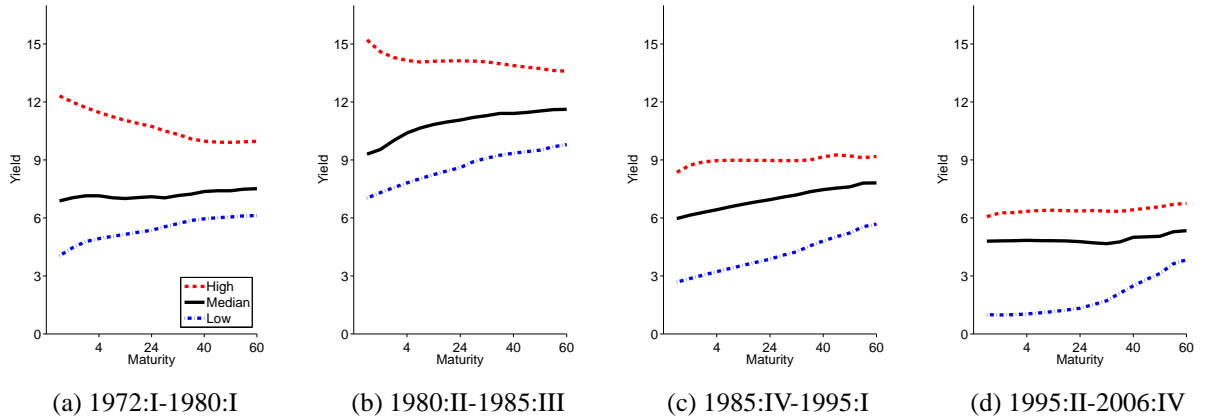


Figure 1: Term structure of interest rates. *Data summary of the term-structure - data obtained from <http://www.federalreserve.gov/econresdata/researchdata.htm>. The graphs display the 5%, 50% and 95% quantiles of the yield curve for bonds of maturity 1, 2, 3, 4, 5, 6, 7, 8, 10, 12, 16, 20, 24, 28, 36 and 40 quarters.*

The rest of the paper is organized as follows. In Section 2 we present our change point term-structure model and derive the resulting bond prices. We outline the prior-posterior analysis of our model in Section 3, deferring details of the MCMC simulation procedure to the appendix of the paper. Section 4 deals with the empirical analysis of the real data and Section 5 has our conclusions.

2 Model Specification

In this section we develop our model of bond pricing under regime changes. Essentially, we will explain the dynamics of bond prices in terms of the evolution of a discrete time, discrete-state variable $\{s_t\}$ that takes one of the values $\{1, 2, \dots, m + 1\}$ such that $s_t = j$ indicates that the time t observation has been drawn from the j th regime, and in terms of the evolution of three continuous factors \mathbf{f}_t consisting of one latent variable u_t and two observed macroeconomic variables \mathbf{m}_t . Let $P_t(s_t, \tau)$ denote the price of the bond at time t in regime s_t that matures in period $(t + \tau)$. Then, under risk-neutral (or arbitrage-free) pricing, we have that

$$P_t(s_t, \tau) = \mathbf{E}_t [\kappa_{t, s_t, t+1} P_{t+1}(s_{t+1}, \tau - 1)] \quad (2.1)$$

where \mathbf{E}_t is the expectation over $(\mathbf{f}_{t+1}, s_{t+1})$, conditioned on (\mathbf{f}_t, s_t) , under the physical measure, and $\kappa_{t,s_t,t+1}$ is the stochastic discount factor (SDF) that converts a time $(t+1)$ payoff into a payoff at time t in regime s_t .

Our goal now is to characterize the stochastic evolution of s_t and the factors \mathbf{f}_t and describe our model of the SDF $\kappa_{t,s_t,t+1}$ in terms of the short-rate process and the market price of factor risks. Given these ingredients, we then derive the prices of our default-free zero coupon bonds that satisfy the preceding condition.

2.1 Change Point Process

We assume that the process of regime-changes is governed by $s_t \in \{1, 2, \dots, m+1\}$. When $s_t = j$, the t th observation is assumed to be drawn from regime j . We refer to the times $\{t_1, t_2, \dots, t_m\}$ at which s_t jumps from one value to the next as the change-points. We will suppose that the parameters in the $(m+1)$ regimes induced by these m change-points are different. As mentioned in Section 1, we describe the stochastic evolution of s_t in terms of a change point instead of a Markov switching process. In this we follow Chib (1998). We suppose that from one time period to the next s_t can either stay at the current value j or jump to the next higher value $(j+1)$. In this sense $\{s_t\}$ can be viewed as a unidirectional process. Thus, in this formulation, return visits to a previously occupied state are not possible. Then, it follows that the j th change point occurs at time (say) t_j when $s_{t_j-1} = j$ and $s_{t_j} = j+1$ ($j = 1, 2, \dots, m$). We further assume that s_t follows a Markov process with transition probabilities given by

$$\mathbf{P} = \begin{bmatrix} p_{11} & 1-p_{11} & 0 & \cdots & 0 \\ 0 & p_{22} & 1-p_{22} & \cdots & 0 \\ 0 & 0 & p_{33} & & 0 \\ \vdots & \vdots & & \ddots & \\ 0 & 0 & 0 & & p_{m+1,m+1} \end{bmatrix} \quad (2.2)$$

where $p_{jk} = \Pr[s_{t+1} = k | s_t = j]$ and, $p_{jk} = 1 - p_{jj}$, $k = j+1$ and $p_{m+1,m+1} = 1$ ($j = 1, 2, \dots, m$).

A feature of this specification is an absorbing terminal state. This is intentional because in any setting with a finite observation window one must have an upper limit on the number of change-points (equivalently, the number of possible regimes). An upper limit on the number of change-points does not rule out, however, the possibility of breaks

beyond the observation window. Although such breaks can occur it is not possible to make inferences about them from the sample data without making consequential and unverifiable assumptions.

An interesting point is that we can assume that the (infinitely lived) economic agents face a possible infinity of change-points. Regardless of the number of change points, however, as is typical in finance and economic theorizing, we assume that these agents know the parameters in the various regimes. Furthermore, in the asset pricing context, we assume that these agents know the current value of the state variable. The central uncertainty from the perspective of these agents is that the state of the next period is random - either the current regime continues or the next possible regime emerges.

This formulation of the change point model in terms of a restricted unidirectional Markov process facilitates bond pricing (as we show below). It also makes obvious how the change point assumption differs from the Markov-switching regime process in Dai et al. (2007), Bansal and Zhou (2002) and Ang et al. (2008) where the transition probability matrix is unrestricted and previously occupied states can be revisited. As we have argued above, there are strong reasons for looking at the term structure from the change point perspective.

2.2 Factor Process

Next, we suppose that the distribution of \mathbf{f}_{t+1} , conditioned on $(\mathbf{f}_t, s_t, s_{t+1})$, is determined by a Gaussian regime-specific mean-reverting first-order autoregression given by

$$\mathbf{f}_{t+1} = \boldsymbol{\mu}_{s_{t+1}} + \mathbf{G}_{s_{t+1}}(\mathbf{f}_t - \boldsymbol{\mu}_{s_t}) + \boldsymbol{\eta}_{t+1} \quad (2.3)$$

where on letting $\mathcal{N}_3(\cdot, \cdot)$ denote the 3-dimensional normal distribution, $\boldsymbol{\eta}_{t+1}|s_{t+1} \sim \mathcal{N}_3(\mathbf{0}, \boldsymbol{\Omega}_{s_{t+1}})$, and for s_t and s_{t+1} ranging from $j = 1$ to $m + 1$, $\boldsymbol{\mu}_j$ is a 3×1 vector and \mathbf{G}_j is a 3×3 matrix. In the sequel, we will express $\boldsymbol{\eta}_{t+1}$ in terms of a vector of i.i.d. standard normal variables $\boldsymbol{\omega}_{t+1}$ as

$$\boldsymbol{\eta}_{t+1} = \mathbf{L}_{s_{t+1}}\boldsymbol{\omega}_{t+1} \quad (2.4)$$

where $\mathbf{L}_{s_{t+1}}$ is the lower-triangular Cholesky decomposition of $\boldsymbol{\Omega}_{s_{t+1}}$.

Thus, the factor evolution is a function of the current and previous states (in contrast, the dynamics in Dai et al. (2007) depend only on s_t whereas those in Bansal and Zhou

(2002) and Ang et al. (2008) depend only on s_{t+1}). This means that the expectation of \mathbf{f}_{t+1} conditioned on $(\mathbf{f}_t, s_t = j, s_{t+1} = k)$ is a function of both $\boldsymbol{\mu}_j$ and $\boldsymbol{\mu}_k$. The appearance of $\boldsymbol{\mu}_j$ in this expression is natural because one would like the autoregression at time $(t + 1)$ to depend on the deviation of \mathbf{f}_t from the regime in the previous period. Of course, the parameter $\boldsymbol{\mu}_j$ can be interpreted as the expectation of \mathbf{f}_{t+1} when regime j is persistent. The matrices $\{\mathbf{G}_j\}$ can also be interpreted in the same way as the mean-reversion parameters in regime j .

2.3 Stochastic Discount Factor

We complete our modeling by assuming that the SDF $\kappa_{t,s_t,t+1}$ that converts a time $(t+1)$ payoff into a payoff at time t in regime s_t is given by

$$\kappa_{t,s_t,t+1} = \exp\left(-r_{t,s_t} - \frac{1}{2}\boldsymbol{\gamma}'_{t,s_t}\boldsymbol{\gamma}_{t,s_t} - \boldsymbol{\gamma}'_{t,s_t}\boldsymbol{\omega}_{t+1}\right) \quad (2.5)$$

where r_{t,s_t} is the short-rate in regime s_t , $\boldsymbol{\gamma}_{t,s_t}$ is the vector of time-varying and regime-sensitive market prices of factor risks and $\boldsymbol{\omega}_{t+1}$ is the i.i.d. vector of regime independent factor shocks in (2.4). The SDF is independent of s_{t+1} given s_t as in the model of Dai et al. (2007).

We suppose that the short rate is affine in the factors and of the form

$$r_{t,s_t} = \delta_{1,s_t} + \boldsymbol{\delta}'_{2,s_t}(\mathbf{f}_t - \boldsymbol{\mu}_{s_t}) \quad (2.6)$$

where the intercept δ_{1,s_t} varies by regime to allow for shifts in the level of the term structure. The multiplier $\boldsymbol{\delta}_{2,s_t} : 3 \times 1$ is also regime-dependent in order to capture shifts in the effects of the macroeconomic factors on the term structure. This is similar to the assumption in Bansal and Zhou (2002) but a departure from both Ang et al. (2008) and Dai et al. (2007) where the coefficient on the factors is constant across regimes. A consequence of our assumption is that the bond prices that satisfy the risk-neutral pricing condition can only be obtained approximately. The same difficulty arises in the work of Bansal and Zhou (2002).

We also assume that the dynamics of $\boldsymbol{\gamma}_{t,s_t}$ are governed by

$$\boldsymbol{\gamma}_{t,s_t} = \tilde{\boldsymbol{\gamma}}_{s_t} + \boldsymbol{\Phi}_{s_t}(\mathbf{f}_t - \boldsymbol{\mu}_{s_t}) \quad (2.7)$$

where $\tilde{\gamma}_{s_t} : 3 \times 1$ is the regime-dependent expectation of γ_{t,s_t} and $\Phi_{s_t} : 3 \times 3$ is a matrix of regime-specific parameters. We refer to the collection $(\tilde{\gamma}_{s_t}, \Phi_{s_t})$ as the factor-risk parameters. Note that in this specification γ_{t,s_t} is the same across maturities but different across regimes. A point to note is that negative market prices of risk have the effect of generating a positive term premium. This is important to keep in mind when we construct the prior distribution on the risk parameters.

It is easily checked that $\mathbf{E}[\kappa_{t,s_t,t+1} | \mathbf{f}_t, s_t = j]$ is equal to the price of a zero coupon bond with $\tau = 1$:

$$\begin{aligned} \mathbf{E}[\kappa_{t,s_t,t+1} | \mathbf{f}_t, s_t = j] &= \sum_{s_{t+1}=j}^{j+1} p_{j s_{t+1}} \mathbf{E}[\kappa_{t,s_t,t+1} | \mathbf{f}_t, s_t = j, s_{t+1}] \\ &= \exp(-r_{t,j}), \quad j \in \{1, 2, \dots, m\} \end{aligned} \quad (2.8)$$

In other words, the SDF satisfies the intertemporal no-arbitrage condition (Dai et al. (2007)).

We note that regime-shift risk is equal to zero in our version of the SDF. We make this assumption because it is difficult to identify this risk from our change-point model where each regime-shift occurs once. Regime risk cannot also be isolated in the models of Ang et al. (2008) and Bansal and Zhou (2002) for the reason that it is confounded with the market price of factor risk.

2.4 Bond Prices

Under these assumptions, we now solve for bond prices that satisfy the risk-neutral pricing condition

$$P_t(s_t, \tau) = \mathbf{E}_t[\kappa_{t,s_t,t+1} P_{t+1}(s_{t+1}, \tau - 1)] \quad (2.9)$$

Following Duffie and Kan (1996), we assume that $P_t(s_t, \tau)$ is a regime-dependent exponential affine function of the factors taking the form

$$P_t(s_t, \tau) = \exp(-\tau R_{\tau t}) \quad (2.10)$$

where $R_{\tau t}$ is the continuously compounded yield given by

$$R_{\tau t} = \frac{1}{\tau} a_{s_t}(\tau) + \frac{1}{\tau} \mathbf{b}_{s_t}(\tau)'(\mathbf{f}_t - \boldsymbol{\mu}_{s_t}) \quad (2.11)$$

and $a_{s_t}(\tau)$ is a scalar function and $\mathbf{b}_{s_t}(\tau)$ is a 3×1 vector of functions, both depending on s_t and τ .

We find the expressions for the latter functions by the method of undetermined coefficients. By the law of the iterated expectation, the risk-neutral pricing formula in (2.9) can be expressed as

$$\mathbf{1} = \mathbf{E}_t \left\{ \mathbf{E}_{t, s_{t+1}} \left[\kappa_{t, s_t, t+1} \frac{P_{t+1}(s_{t+1}, \tau - 1)}{P_t(s_t, \tau)} \right] \right\} \quad (2.12)$$

where the inside expectation $\mathbf{E}_{t, s_{t+1}}$ is conditioned on s_{t+1} , s_t and \mathbf{f}_t . Subsequently, as discussed in Appendix A, one now substitutes $P_t(s_t, \tau)$ and $P_{t+1}(s_{t+1}, \tau - 1)$ from (2.10) and (2.11) into this expression, and integrate out s_{t+1} after a log-linearization. We match common coefficients and solve for the unknown functions. When $j \in \{1, \dots, m\}$ and $k = j + 1$, this procedure produces the following recursive system for the unknown functions

$$\begin{aligned} a_j(\tau) &= \begin{pmatrix} p_{jj} & p_{jk} \end{pmatrix} \begin{pmatrix} \delta_{1,j} - \tilde{\gamma}_j \mathbf{L}'_j \mathbf{b}_j(\tau - 1) - \mathbf{b}_j(\tau - 1)' \mathbf{L}_j \mathbf{L}'_j \mathbf{b}_j(\tau - 1)/2 + a_j(\tau - 1) \\ \delta_{1,j} - \tilde{\gamma}_j \mathbf{L}'_k \mathbf{b}_k(\tau - 1) - \mathbf{b}_k(\tau - 1)' \mathbf{L}_k \mathbf{L}'_k \mathbf{b}_k(\tau - 1)/2 + a_k(\tau - 1) \end{pmatrix} \\ \mathbf{b}_j(\tau) &= \begin{pmatrix} p_{jj} & p_{jk} \end{pmatrix} \begin{pmatrix} \boldsymbol{\delta}_{2,j} + (\mathbf{G}_j - \mathbf{L}_j \Phi_j)' \mathbf{b}_j(\tau - 1) \\ \boldsymbol{\delta}_{2,j} + (\mathbf{G}_k - \mathbf{L}_k \Phi_j)' \mathbf{b}_k(\tau - 1) \end{pmatrix} \end{aligned} \quad (2.13)$$

where τ runs over the positive integers. These recursions are initialized by setting $a_{s_t}(0) = 0$ and $\mathbf{b}_{s_t}(0) = \mathbf{0}_{3 \times 1}$ for all s_t . It is readily seen that the resulting intercept and factor loadings are determined by the weighted average of the two potential realizations in the next period where the weights are given by the transition probabilities p_{jj} and $(1 - p_{jj})$, respectively. Thus, the bond prices in regime $s_t = j$ ($j \leq m$) incorporate the expectation that the economy in the next period will continue to stay in regime j , or that it will switch to the next possible regime $k = j + 1$, each weighted with the probabilities p_{jj} and $1 - p_{jj}$, respectively.

Note that when we consider inference with a given sample of data, and the number of change points m is a finite number, the above recursions are supplemented by the expressions

$$\begin{aligned} a_j(\tau) &= \delta_{1,j} - \tilde{\gamma}_j \mathbf{L}'_j \mathbf{b}_j(\tau - 1) - \mathbf{b}_j(\tau - 1)' \mathbf{L}_j \mathbf{L}'_j \mathbf{b}_j(\tau - 1)/2 + a_j(\tau - 1) \\ \mathbf{b}_j(\tau) &= \boldsymbol{\delta}_{2,j} + (\mathbf{G}_j - \mathbf{L}_j \Phi_j)' \mathbf{b}_j(\tau - 1) \end{aligned} \quad (2.14)$$

for $j = m + 1$.

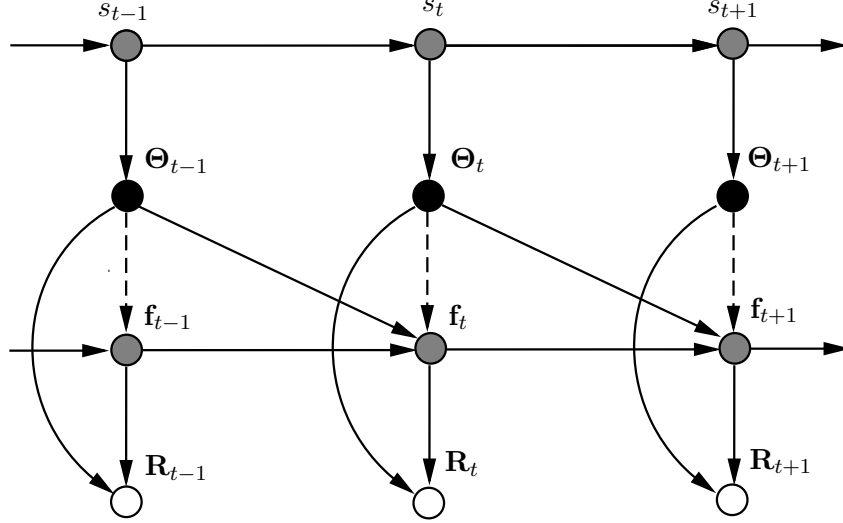


Figure 2: Directed graph of model linkages.

Figure 2 summarizes the economy that we have just described in terms of a directed acyclic graph. In the beginning of period t , a regime realization occurs. This realization is governed with the regime in the previous period as indicated by the direction of the arrow connecting s_{t-1} to s_t . Then given the regime at time t , the corresponding model parameters Θ_t are taken from the full collection of model parameters. These determine the functions $a_{s_t}(\tau)$ and $\mathbf{b}_{s_t}(\tau)$ according to the recursions in (2.13) and (2.14). Conditioned on the parameters and \mathbf{f}_{t-1} , \mathbf{f}_t is generated by the regime-specific autoregressive process in (2.3). Finally, from (2.11), $a_{s_t}(\tau)$, $\mathbf{b}_{s_t}(\tau)$ and \mathbf{f}_t determine the yields of all maturities. Notice that in Dai et al. (2007) the dashed line in figure 2 is absent since \mathbf{f}_t is assumed to be drawn independently of s_t .

2.5 Regime-specific Term Premium

As is well known, under risk-neutral pricing, after adjusting for risk, agents are indifferent between holding a τ -period bond and a risk-free bond for one period. The risk adjustment is the term premium. In the regime-change model, this term-premium is regime specific. For each time t and in the current regime $s_t = j$, the term-premium for a τ -period bond can be calculated as

$$\text{Term-premium}_{\tau,t,s_t} = (\tau - 1)\text{Cov}(\ln \kappa_{t,s_t,t+1}, R_{\tau-1,t+1} | \mathbf{f}_t, s_t = j) \quad (2.15)$$

$$= -p_{jj}\mathbf{b}_j(\tau - 1)' \mathbf{L}_j \boldsymbol{\gamma}_{t,j} - p_{jk}\mathbf{b}_k(\tau - 1)' \mathbf{L}_k \boldsymbol{\gamma}_{t,j}$$

where $k = j + 1$. One can see that if \mathbf{L}_j , which quantifies the size of the factor shocks in the current regime $s_t = j$, is large, or if $\boldsymbol{\gamma}_{t,j}$, the market prices of factor risk, is highly negative, then the term premium is expected to be large. Even if \mathbf{L}_j in the current regime is small, one can see from the second term in the above expression that the term premium can be big if the probability of jumping to the next possible regime is high and \mathbf{L}_k in that regime is large. In our empirical implementation we calculate this regime-specific term premium for each time period in the sample.

3 Estimation and Inference

In this section we consider the empirical implementation of our yield curve model. In order to get a detailed perspective of the yield curve and its dynamics over time we operationalize our pricing model on a data set of 16 yields of US T-bills measured quarterly between 1972: I and 2007: IV on the maturities given by

$$\{1, 2, 3, 4, 5, 6, 7, 8, 10, 12, 16, 20, 24, 28, 36, 40\}$$

quarters. As far as we know, this is the largest number of yields that have been considered in the setting of affine yield curve models. For these data, we consider five versions of our general model, with 0, 1, 2, 3 and 4 change points and denoted by $\{\mathcal{M}_m\}_{m=0}^4$. The largest model that we fit, namely \mathcal{M}_4 , has a total of 209 free parameters. We fit these various models by tuned Bayesian methods as we discuss below and then compare the competing models through marginal likelihoods, Bayes factors and the predictive performance out of sample.

To begin, let the 16 yields under study be denoted by

$$(R_{1t}, R_{2t}, \dots, R_{16t})', \quad t = 1, 2, \dots, n, \quad (3.1)$$

where $R_{it} = R_{\tau_i, t}$ and τ_i is the i th maturity (in quarters), and let the two macro factors be denoted by

$$\mathbf{m}_t = (m_{1t}, m_{2t}), \quad t = 1, 2, \dots, n$$

where m_{1t} is the inflation rate and m_{2t} is the real GDP growth rate. We also let

$$\mathbf{S}_n = \{s_t\}_{t=1}^n$$

denote the sequence of (unobserved) regime indicators.

We now specify the set of model parameters to be estimated. First, the unknown elements of \mathbf{G}_{s_t} and Φ_{s_t} are denoted by

$$\mathbf{g}_{s_t} = \{G_{ij,s_t}\}_{i,j=1,2,3} \text{ and } \phi_{s_t} = \{\Phi_{jj,s_t}\}_{j=1,2,3}$$

where G_{ij,s_t} and Φ_{ij,s_t} denote the (i, j) th element of \mathbf{G}_{s_t} and Φ_{s_t} , respectively. The unknown elements of Ω_{s_t} are defined as

$$\boldsymbol{\lambda}_{s_t} = \{l_{21,s_t}, l_{22,s_t}^*, l_{31,s_t}, l_{32,s_t}, l_{33,s_t}^*\}$$

where these are obtained from the decomposition $\Omega_{s_t} = \mathbf{L}_{s_t} \mathbf{L}'_{s_t}$ with \mathbf{L}_{s_t} expressed as

$$\begin{pmatrix} 1/400 & 0 & 0 \\ l_{21,s_t} & \exp(l_{22,s_t}^*) & 0 \\ l_{31,s_t} & l_{32,s_t} & \exp(l_{33,s_t}^*) \end{pmatrix} \quad (3.2)$$

The elements of $\boldsymbol{\lambda}_{s_t}$ are unrestricted. Next, the parameters of the short-rate equation are expressed as $\boldsymbol{\delta}_{s_t} = (\delta_{1,s_t} \times 400, \boldsymbol{\delta}'_{2,s_t})'$ and those in the transition matrix \mathbf{P} by $\mathbf{p} = \{p_{jj}, j = 1, 2, \dots, m\}$. Finally, the unknown pricing error variances σ_{i,s_t}^2 are collected in reparameterized form as

$$\boldsymbol{\sigma}^{*2} = \{\sigma_{i,s_t}^{*2} = d_i \sigma_{i,s_t}^2, i = 1, \dots, 7, 8, \dots, 16 \text{ and } s_t = 1, 2, \dots, m + 1\}$$

where $d_1 = 30, d_2 = d_{16} = 40, d_3 = d_{12} = 200, d_4 = 350, d_5 = d_6 = d_{11} = 500, d_7 = 3000, d_9 = 1500, d_{10} = 1000, d_{13} = d_{14} = d_{15} = 200$. These positive multipliers are introduced to increase the magnitude of the variances.

Under these notations, for any given model with m change-points, the parameters of interest can be denoted as $\boldsymbol{\psi} = (\boldsymbol{\theta}, \boldsymbol{\sigma}^{*2}, u_0)$ where

$$\boldsymbol{\theta} = \{\mathbf{g}_{s_t}, \boldsymbol{\mu}_{m,s_t}, \boldsymbol{\delta}_{s_t}, \tilde{\boldsymbol{\gamma}}_{s_t}, \phi_{s_t}, \boldsymbol{\lambda}_{s_t}, \mathbf{p}\}_{s_t=1}^{m+1}$$

and u_0 is the latent factor at time 0. Note that to economize on notation, we do not index these parameters by a model subscript.

3.1 Joint distribution of the yields and macro factors

We now derive the joint distribution of the yields and the macro factors conditioned on \mathbf{S}_n and $\boldsymbol{\psi}$. This joint distribution can be obtained without marginalization over $\{u_t\}_{t=1}^n$

if we assume (following, for example, Chen and Scott (2003) and Dai et al. (2007)) that one of the yields is priced exactly without error. This is the so-called basis yield. Under this assumption the latent factor can be expressed in terms of the observed variables and eliminated from the model, as we now describe.

Assume that R_{8t} (the eighth yield in the list above) is the basis yield which is priced exactly by the model. Let \mathbf{R}_t denote the remaining 15 yields (which are measured with pricing error). Define $\bar{a}_{i,s_t} = a_{s_t}(\tau_i)/\tau_i$ and $\bar{\mathbf{b}}_{i,s_t} = \mathbf{b}_{s_t}(\tau_i)/\tau_i$ where $a_{s_t}(\tau_i)$ and $\mathbf{b}_{s_t}(\tau_i)$ are obtained from the recursive equations in (2.13) - (2.14). Also let \bar{a}_{8,s_t} ($\bar{\mathbf{a}}_{s_t}$) and $\bar{\mathbf{b}}_{8,s_t}$ ($\bar{\mathbf{b}}_{s_t}$) be the corresponding intercept and factor loadings for R_{8t} (\mathbf{R}_t), respectively. Then, since the basis yield is priced without error, if we let

$$\bar{\mathbf{b}}_{8,s_t} = \begin{pmatrix} \bar{b}_{8,u,s_t} \\ \bar{\mathbf{b}}_{8,m,s_t} \end{pmatrix} \quad (3.3)$$

we can see from (2.11) that R_{8t} is given by

$$R_{8t} = \bar{a}_{8,s_t} + \bar{b}_{8,u,s_t}u_t + \bar{\mathbf{b}}'_{8,m,s_t}(\mathbf{m}_t - \boldsymbol{\mu}_{m,s_t}) \quad (3.4)$$

On rewriting this expression, it follows that u_t is

$$u_t = (\bar{b}_{8,u,s_t})^{-1} (R_{8t} - \bar{a}_{8,s_t} - \bar{\mathbf{b}}'_{8,m,s_t}(\mathbf{m}_t - \boldsymbol{\mu}_{m,s_t})) \quad (3.5)$$

Conditioned on \mathbf{m}_t and s_t , this represents a one-to-one map between R_{8t} and u_t . If we let

$$\mathbf{z}_t = \begin{pmatrix} R_{8t} \\ \mathbf{m}_t \end{pmatrix},$$

$$\alpha_{s_t} = \begin{pmatrix} (\bar{b}_{8,u,s_t})^{-1} \bar{\mathbf{b}}'_{8,m,s_t} \boldsymbol{\mu}_{m,s_t} - (\bar{b}_{8,u,s_t})^{-1} \bar{a}_{8,s_t} \\ \mathbf{0}_{2 \times 1} \end{pmatrix}, \text{ and} \quad (3.6)$$

$$\mathbf{A}_{s_t} = \begin{pmatrix} (\bar{b}_{8,u,s_t})^{-1} & -(\bar{b}_{8,u,s_t})^{-1} \bar{\mathbf{b}}'_{8,m,s_t} \\ \mathbf{0}_{2 \times 1} & \mathbf{I}_2 \end{pmatrix}$$

then one can check that \mathbf{f}_t can be expressed as

$$\mathbf{f}_t = \alpha_{s_t} + \mathbf{A}_{s_t} \mathbf{z}_t \quad (3.7)$$

It now follows from equation (2.11) that conditioned on \mathbf{z}_t (equivalently \mathbf{f}_t), s_t and the model parameters $\boldsymbol{\psi}$, the non-basis yields \mathbf{R}_t in our model are generated according to the process

$$\mathbf{R}_t = \bar{\mathbf{a}}_{s_t} + \bar{\mathbf{b}}_{s_t}(\mathbf{f}_t - \boldsymbol{\mu}_{s_t}) + \boldsymbol{\varepsilon}_t, \quad \boldsymbol{\varepsilon}_t \sim \text{iid}\mathcal{N}(0, \boldsymbol{\Sigma}_{s_t}) \quad (3.8)$$

where

$$\Sigma_{s_t} = \text{diag}(\sigma_{1,s_t}^2, \sigma_{2,s_t}^2, \dots, \sigma_{7,s_t}^2, \sigma_{9,s_t}^2, \dots, \sigma_{16,s_t}^2).$$

In other words,

$$\begin{aligned} p(\mathbf{R}_t | \mathbf{z}_t, s_t, \boldsymbol{\psi}) &= p(\mathbf{R}_t | \mathbf{f}_t, s_t, \boldsymbol{\psi}) \\ &= \mathcal{N}_{15}(\mathbf{R}_t | \bar{\mathbf{a}}_{s_t} + \bar{\mathbf{b}}_{s_t}(\mathbf{f}_t - \boldsymbol{\mu}_{s_t}), \Sigma_{s_t}) \end{aligned} \quad (3.9)$$

In addition, the distribution of \mathbf{z}_t conditioned on \mathbf{z}_{t-1} , s_t and s_{t-1} is obtained straightforwardly from the process generating \mathbf{f}_t given in equation (2.3) and the linear map between \mathbf{f}_t and \mathbf{z}_t given in equation (3.7). In particular,

$$\begin{aligned} p(\mathbf{z}_t | \mathbf{z}_{t-1}, s_t, s_{t-1}, \boldsymbol{\psi}) &= p(\mathbf{f}_t | \mathbf{f}_{t-1}, s_t, s_{t-1}, \boldsymbol{\psi}) \det(\mathbf{A}_{s_t}) \\ &= \mathcal{N}_3(\boldsymbol{\mu}_{s_t} + \mathbf{G}_{s_t}(\mathbf{f}_{t-1} - \boldsymbol{\mu}_{s_{t-1}}), \Omega_{s_t}) | (\bar{b}_{8,u,s_t})^{-1} | \end{aligned} \quad (3.10)$$

If we let

$$\mathbf{y}_t = (\mathbf{R}_t, \mathbf{z}_t) \text{ and } \mathbf{y} = \{\mathbf{y}_t\}_{t=1}^n$$

it follows that the required joint density of \mathbf{y} conditioned on $(\mathbf{S}_n, \boldsymbol{\psi})$ is given by

$$p(\mathbf{y} | \mathbf{S}_n, \boldsymbol{\psi}) = \prod_{t=1}^n \mathcal{N}_{15}(\mathbf{R}_t | \bar{\mathbf{a}}_{s_t} + \bar{\mathbf{b}}_{s_t}(\mathbf{f}_t - \boldsymbol{\mu}_{s_t}), \Sigma_{s_t}) \quad (3.11)$$

$$\times \mathcal{N}_3(\boldsymbol{\mu}_{s_t} + \mathbf{G}_{s_t}(\mathbf{f}_{t-1} - \boldsymbol{\mu}_{s_{t-1}}), \Omega_{s_t}) | (\bar{b}_{8,u,s_t})^{-1} | \quad (3.12)$$

3.2 Prior Distribution

Because of the size of the parameter space, and the complex cross-maturity restrictions on the parameters, the formulation of the prior distribution can be a challenge. Chib and Ergashev (2009) have tackled this problem and shown that a reasonable approach for constructing the prior is to think in terms of the term structure that is implied by the prior distribution. The implied yield curve can be determined by simulation: simulating parameters from the prior and simulating yields from the model given the parameters. The prior can be adjusted until the implied term structure is viewed as satisfactory on a priori considerations. Chib and Ergashev (2009) use this strategy to arrive at a prior distribution that incorporates the belief of a positive term premium and stationary but persistent factors. We adapt their approach for our model with change-points, ensuring

that the yield curve implied by our prior distribution is upward sloping. We assume, in addition, that the prior distribution of the regime specific parameters is identical across regimes. We arrive at our prior distribution in this way for each of the five models we consider - with 0, 1, 2, 3 and 4 change-points.

We begin by recalling the identifying restrictions on the parameters. First, we set $\boldsymbol{\mu}_{u,s_t} = 0$ which implies that the mean of the short rate conditional on s_t is δ_{1,s_t} . Next, the first element of $\boldsymbol{\delta}_{2,s_t}$, namely δ_{21,s_t} , is assumed to be non-negative. Finally, to enforce stationarity of the factor process, we restrict the eigenvalues of \mathbf{G}_{s_t} to lie inside the unit circle. Thus, under the physical measure, the factors are mean reverting in each regime. These constraints are summarized as

$$\mathcal{R} = \{\mathbf{G}_j, \delta_{21,j} | \delta_{21,j} \geq 0, 0 \leq p_{jj} \leq 1, |eig(\mathbf{G}_j)| < 1 \text{ for } j = 1, 2, \dots, m+1\} \quad (3.13)$$

All the constraints in \mathcal{R} are enforced through the prior distribution.

The free parameters in $\boldsymbol{\theta}$ and $\boldsymbol{\sigma}^{*2}$ are assumed to be mutually independent. Our prior distribution on $\boldsymbol{\theta}$ is normal $\mathcal{N}(\bar{\boldsymbol{\theta}}, \bar{\mathbf{V}}_{\boldsymbol{\theta}})$ truncated by the restrictions in \mathcal{R} . In particular, the $\mathcal{N}(\bar{\boldsymbol{\theta}}, \bar{\mathbf{V}}_{\boldsymbol{\theta}})$ distribution has the form

$$\begin{aligned} & \prod_{s_t=1}^m \mathcal{N}(p_{s_t s_t} | \bar{p}_{s_t s_t}, \bar{\mathbf{V}}_{p_{s_t s_t}}) \\ & \times \prod_{s_t=1}^{m+1} \left\{ \mathcal{N}(\mathbf{g}_{s_t} | \bar{\mathbf{g}}_{s_t}, \bar{\mathbf{V}}_{\mathbf{g}_{s_t}}) \mathcal{N}(\boldsymbol{\mu}_{m,s_t} | \bar{\boldsymbol{\mu}}_{m,s_t}, \bar{\mathbf{V}}_{\boldsymbol{\mu}_{m,s_t}}) \mathcal{N}(\boldsymbol{\delta}_{s_t} | \bar{\boldsymbol{\delta}}_{s_t}, \bar{\mathbf{V}}_{\boldsymbol{\delta}_{s_t}}) \right\} \\ & \times \prod_{s_t=1}^{m+1} \left\{ \mathcal{N}(\tilde{\boldsymbol{\gamma}}_{s_t} | \bar{\tilde{\boldsymbol{\gamma}}}_{s_t}, \bar{\mathbf{V}}_{\tilde{\boldsymbol{\gamma}}_{s_t}}) \mathcal{N}(\boldsymbol{\phi}_{s_t} | \bar{\boldsymbol{\phi}}_{s_t}, \bar{\mathbf{V}}_{\boldsymbol{\phi}_{s_t}}) \mathcal{N}(\lambda_{s_t} | \bar{\lambda}_{s_t}, \bar{\mathbf{V}}_{\lambda_{s_t}}) \right\} \end{aligned}$$

which we explain as follows.

First, the prior on p_{jj} ($j = 1, \dots, m$) is normal with a standard deviation of 0.33, truncated to the interval (0, 1). The mean of these distributions is model-specific. For example, in the \mathcal{M}_1 model, the mean is 0.986, so that the a priori expected duration of stay in regime 1 is about 70 quarters in relation to a sample period of 140 quarters. In the \mathcal{M}_2 , \mathcal{M}_3 and \mathcal{M}_4 models, the prior mean of the transition probabilities is specified to imply 50, 40 and 33 quarters of expected duration in each regime. It is important to note that we work with a truncated normal prior distribution on these transition probabilities instead of the more conventional beta distribution because $\bar{\mathbf{a}}_{s_t}$ and $\bar{\mathbf{b}}_{s_t}$ in

the equation (3.8) are a function of p_{jj} , which eliminates any benefit from the use of a beta functional form. *Second*, we construct $\bar{\mathbf{g}}_{s_t}$ from the matrix

$$\bar{\mathbf{G}}_{s_t} = \text{diag}(0.95, 0.8, 0.4)$$

and let $\bar{\mathbf{V}}_{\mathbf{g}_{s_t}}$ be a diagonal matrix with each diagonal element equal to 0.1. This choice of prior incorporates the prior belief that the latent factor is more persistent than the macro factors. *Third*, we assume that $\bar{\boldsymbol{\mu}}_{m,s_t} \times 400 = (4, 3)'$ and $\bar{\mathbf{V}}_{\boldsymbol{\mu}_{m,s_t}} \times 400^2 = \text{diag}(25, 1)$. Thus, the prior mean of inflation is assumed to be 4% and that of real GDP growth rate to be 3%. The standard deviations of 5% and 1% produces a distribution that covers the most likely values of these rates. *Fourth*, based on the Taylor rule intuition that the response of the short rate to an increase of inflation and output growth tend to be positive, we let

$$\bar{\boldsymbol{\delta}}_{s_t} = (6, 0.8, 0.4, 0.4)$$

and the let the prior standard deviations be $(5, 0.4, 0.4, 0.4)$. *Fifth*, we assume that

$$\bar{\boldsymbol{\gamma}}_{s_t} = (-0.5, -0.5, -0.5) \text{ and } \bar{\mathbf{V}}_{\boldsymbol{\gamma}_{s_t}} = \text{diag}(0.1, 0.1, 0.1)$$

where the prior mean of $\tilde{\boldsymbol{\gamma}}_{s_t}$ is negative in order to suggest an upward sloping average yield curve in each regime. *Sixth*, we assume that

$$\bar{\boldsymbol{\phi}}_{s_t} = (1, 1, 1) \text{ and } \bar{\mathbf{V}}_{\boldsymbol{\phi}_{s_t}} = \text{diag}(1, 1, 1)$$

where the positive prior is justified from the intuition that positive shocks to macroeconomic fundamentals should tend to decrease the overall risk in the economy. *Seventh*, we let

$$\bar{\boldsymbol{\lambda}}_{s_t} = (0, 0, 0, 0, 1) \text{ and } \bar{\mathbf{V}}_{\boldsymbol{\lambda}_{s_t}} = \text{diag}(4, 4, 4, 4, 4)$$

which tends to imply reasonable prior variation in the implied yield curve.

Next, we place the prior on the $15 \times m$ free parameters of $\boldsymbol{\sigma}^{*2}$. Each σ_{i,s_t}^{*2} is assumed to have an inverse-gamma prior distribution $\mathcal{IG}(\bar{v}, \bar{d})$ with $\bar{v} = 4.08$ and $\bar{d} = 20.80$ which implies a mean of 10 and standard deviation of 14.

Finally, we assume that the latent factor u_0 at time 0 follows the steady-state distribution in regime 1

$$u_0 \sim \mathcal{N}(0, V_u) \tag{3.14}$$

where $V_u = (1 - G_{11,1}^2)^{-1}$.

To show what these assumptions imply for the outcomes, we simulate the parameters 50,000 times from the prior, and for each drawing of the parameters, we simulate the factors and yields for each maturity and each of 50 quarters. The median, 2.5% and 97.5% quantile surfaces of the resulting term structure in annualized percents are reproduced in Figure 3. Because our prior distribution is symmetric among the regimes, the prior distribution of the yield curve is not regime-specific. It can be seen that the simulated prior term structure is gently upward sloping on average. Also the assumed prior allows for considerable a priori variation in the term structure.

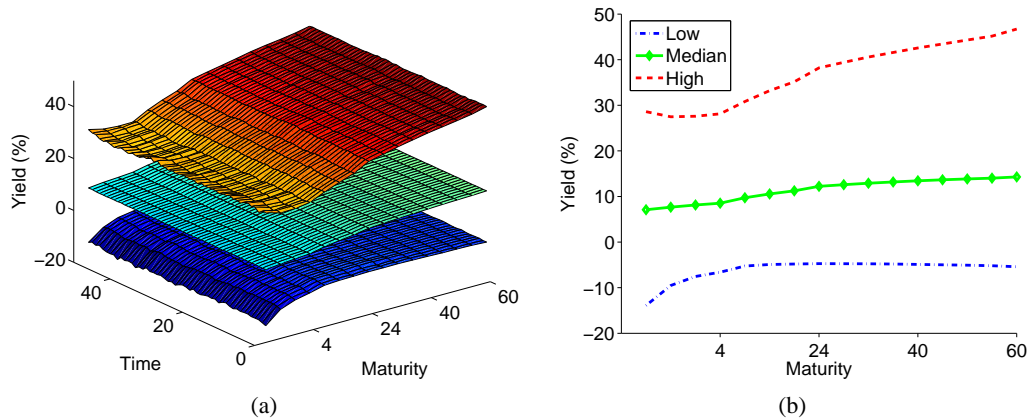


Figure 3: The implied prior term structure dynamics. *These graphs are based on 50,000 simulated draws of the parameters from the prior distribution. In the graphs on the left, the “Low”, “Median”, and “High” surfaces correspond to the 2.5%, 50%, and 97.5% quantile surfaces of the term structure dynamics in annualized percents implied by the prior distribution. In the second graph, the surfaces of the first graph are averaged over the entire period of 50 quarters.*

3.3 Posterior Distribution and MCMC Sampling

Under our assumptions it is now possible to calculate the posterior distribution of the parameters by MCMC simulation methods. Our MCMC approach is grounded in the recent developments that appear in Chib and Ergashev (2009) and Chib and Ramamurthy (2009). The latter paper introduces an implementation of the MCMC method (called the tailored randomized block M-H algorithm) that we adopt here to fit our model. The idea behind this implementation is to update parameters in blocks, where both the number of blocks and the members of the blocks are randomly chosen within

each MCMC cycle. This strategy is especially valuable in high-dimensional problems and in problems where it is difficult to form the blocks on a priori considerations.

The posterior distribution that we would like to explore is given by

$$\pi(\mathbf{S}_n, \boldsymbol{\psi} | \mathbf{y}) \propto p(\mathbf{y} | \mathbf{S}_n, \boldsymbol{\psi}) p(\mathbf{S}_n | \boldsymbol{\psi}) \pi(\boldsymbol{\psi}) \quad (3.15)$$

where $p(\mathbf{y} | \mathbf{S}_n, \boldsymbol{\psi})$ is the distribution of the data given the regime indicators and the parameters, $p(\mathbf{S}_n | \boldsymbol{\psi})$ is the density of the regime-indicators given the parameters and the initial latent factor, and $\pi(\boldsymbol{\psi})$ is the joint prior density of u_0 and the parameters. Note that by conditioning on \mathbf{S}_n we avoid the calculation of the likelihood function $p(\mathbf{y} | \boldsymbol{\psi})$ whose computation is more involved. We discuss the computation of the likelihood function in the next section in connection with the calculation of the marginal likelihood.

The idea behind the MCMC approach is to sample this posterior distribution iteratively, such that the sampled draws form a Markov chain with invariant distribution given by the target density. Practically, the sampled draws after a suitably specified burn-in are taken as samples from the posterior density. We construct our MCMC simulation procedure by sampling various blocks of parameters and latent variables in turn within each MCMC iteration. The distributions of these various blocks of parameters are each proportional to the joint posterior $\pi(\mathbf{S}_n, \boldsymbol{\psi} | \mathbf{y})$. In particular, after initializing the various unknowns, we go through 4 iterative steps in each MCMC cycle. Briefly, in Step 2 we sample $\boldsymbol{\theta}$ from the posterior distribution that is proportional to

$$p(\mathbf{y} | \mathbf{S}_n, \boldsymbol{\psi}) \pi(u_0 | \boldsymbol{\theta}) \pi(\boldsymbol{\theta}) \quad (3.16)$$

The sampling of $\boldsymbol{\theta}$ from the latter density is done by the TaRB-MH method of Chib and Ramamurthy (2009). In Step 3 we sample u_0 from the posterior distribution that is proportional to

$$p(\mathbf{y} | \mathbf{S}_n, \boldsymbol{\psi}) p(\mathbf{S}_n | \boldsymbol{\psi}) \pi(u_0 | \boldsymbol{\theta}) \quad (3.17)$$

In Step 4, we sample \mathbf{S}_n conditioned on $\boldsymbol{\psi}$ in one block by the algorithm of Chib (1996). We finish one cycle of the algorithm by sampling $\boldsymbol{\sigma}^{*2}$ conditioned on $(\mathbf{S}_n, \boldsymbol{\theta})$ from the posterior distribution that is proportional to

$$p(\mathbf{y} | \mathbf{S}_n, \boldsymbol{\psi}) \pi(\boldsymbol{\sigma}^{*2}) \quad (3.18)$$

Our algorithm can be summarized as follows.

Algorithm: MCMC sampling

- Step 1** Initialize $(\mathbf{S}_n, \boldsymbol{\psi})$ and fix n_0 (the burn-in) and n_1 (the MCMC sample size)
- Step 2** Sample $\boldsymbol{\theta}$ conditioned on $(\mathbf{y}, \mathbf{S}_n, u_0, \boldsymbol{\sigma}^{*2})$
- Step 3** Sample u_0 conditioned on $(\mathbf{y}, \boldsymbol{\theta}, \mathbf{S}_n)$
- Step 4** Sample \mathbf{S}_n conditioned on $(\mathbf{y}, \boldsymbol{\theta}, u_0, \boldsymbol{\sigma}^{*2})$
- Step 5** Sample $\boldsymbol{\sigma}^{*2}$ conditioned on $(\mathbf{y}, \boldsymbol{\theta}, \mathbf{S}_n)$
- Step 6** Repeat Steps 2-6, discard the draws from the first n_0 iterations and save the subsequent n_1 draws.

Full details of each of these steps are given in appendix B.

3.4 Marginal Likelihood Computation

One of our goals is to evaluate the extent to which the regime-change model is an improvement over the model without regime-changes. We are also interested in determining how many regimes best describe the sample data. Specifically, we are interested in the comparison of 5 models which in the introduction were named as \mathcal{M}_0 , \mathcal{M}_1 , \mathcal{M}_2 , \mathcal{M}_3 and \mathcal{M}_4 . The most general model is \mathcal{M}_4 that has 4 possible change points, 1 latent factor and 2 macro factors. We do the comparison in terms of marginal likelihoods and their ratios which are called Bayes factors. The marginal likelihood of any given model is obtained as

$$m(\mathbf{y}) = \int p(\mathbf{y}|\mathbf{S}_n, \boldsymbol{\psi})p(\mathbf{S}_n|\boldsymbol{\psi})\pi(\boldsymbol{\psi})d(\mathbf{S}_n, \boldsymbol{\psi}) \quad (3.19)$$

This integration is obviously infeasible by direct means. It is possible, however, by the method of Chib (1995) which starts with the recognition that the marginal likelihood can be expressed in equivalent form as

$$m(\mathbf{y}) = \frac{p(\mathbf{y}|\boldsymbol{\psi}^*)\pi(\boldsymbol{\psi}^*)}{\pi(\boldsymbol{\psi}^*|\mathbf{y})} \quad (3.20)$$

where $\boldsymbol{\psi}^* = (\boldsymbol{\theta}^*, \boldsymbol{\sigma}^{*2}, u_0^*)$ is some specified (say high-density) point of $\boldsymbol{\psi} = (\boldsymbol{\theta}, \boldsymbol{\sigma}^{*2}, u_0)$. Provided we have an estimate of posterior ordinate $\pi(\boldsymbol{\psi}^*|\mathbf{y})$ the marginal likelihood can

be computed on the log scale as

$$\ln \hat{m}(\mathbf{y}) = \ln p(\mathbf{y}|\boldsymbol{\psi}^*) + \ln \pi(\boldsymbol{\psi}^*) - \ln \hat{\pi}(\boldsymbol{\psi}^*|\mathbf{y}) \quad (3.21)$$

Notice that the first term in this expression is the likelihood. It has to be evaluated only at a single point which is highly convenient. The calculation of the second term is straightforward. Finally, the third term is obtained from a marginal-conditional decomposition following Chib (1995). The specific implementation in this context requires the technique of Chib and Jeliazkov (2001) as modified by Chib and Ramamurthy (2009) for the case of randomized blocks.

As for the calculation of the likelihood, the joint density of the data $\mathbf{y} = (\mathbf{y}_1, \dots, \mathbf{y}_n)$ is, by definition,

$$p(\mathbf{y}|\boldsymbol{\psi}) = \sum_{t=0}^{n-1} \ln p(\mathbf{y}_{t+1}|I_t, \boldsymbol{\psi}) \quad (3.22)$$

where

$$p(\mathbf{y}_{t+1}|I_t, \boldsymbol{\psi}) = \sum_{s_{t+1}=1}^{m+1} \sum_{s_t=1}^{m+1} p(\mathbf{y}_{t+1}|I_t, s_t, s_{t+1}, \boldsymbol{\psi}) \Pr[s_t, s_{t+1}|I_t, \boldsymbol{\psi}]$$

is the one-step ahead predictive density of \mathbf{y}_{t+1} , and I_t consists of the history of the outcomes R_t and \mathbf{z}_t up to time t . On the right hand side, the first term is the density of \mathbf{y}_{t+1} conditioned on $(I_t, s_t, s_{t+1}, \boldsymbol{\psi})$ which is given in equation (3.11), whereas the second term can be calculated from the law of total probability as

$$\Pr[s_t = j, s_{t+1} = k|I_t, \boldsymbol{\psi}] = p_{jk} \Pr[s_t = j|I_t, \boldsymbol{\psi}] \quad (3.23)$$

where $\Pr[s_t = j|I_t, \boldsymbol{\psi}]$ is obtained recursively starting with $\Pr[s_1 = 1|I_0, \boldsymbol{\psi}] = 1$ by the following steps. Once \mathbf{y}_{t+1} is observed at the end of time $t + 1$, the probability of the regime $\Pr[s_{t+1} = k|I_t, \boldsymbol{\psi}]$ from the previous step is updated to $\Pr[s_{t+1} = k|I_{t+1}, \boldsymbol{\psi}]$ as

$$\Pr[s_{t+1} = k|I_{t+1}, \boldsymbol{\psi}] = \sum_{j=1}^{m+1} \Pr[s_t = j, s_{t+1} = k|I_{t+1}, \boldsymbol{\psi}] \quad (3.24)$$

where

$$\Pr[s_t = j, s_{t+1} = k|I_{t+1}, \boldsymbol{\psi}] = \frac{p[\mathbf{y}_{t+1}|I_t, s_t = j, s_{t+1} = k, \boldsymbol{\psi}] \Pr[s_t = j, s_{t+1} = k|I_t, \boldsymbol{\psi}]}{p[\mathbf{y}_{t+1}|I_t, \boldsymbol{\psi}]} \quad (3.25)$$

This completes the calculation of the likelihood function.

4 Results

We apply our modeling approach to analyze US data on quarterly yields of sixteen US T-bills between 1972:I and 2007:IV. These data are taken from Gurkaynak, Sack, and Wright (2007). We consider zero-coupon bonds of maturities 1, 2, 3, 4, 5, 6, 7, 8, 10, 12, 16, 20, 24, 28, 36, and 40 quarters. We let the basis yield be the 8 quarter (or 2 year) bond which is the bond with the smallest pricing variance. Our macroeconomic factors are the quarterly GDP inflation deflator and the real GDP growth rate. These data are from the Federal reserve bank of St. Louis.

We work with 16 yields because our tuned Bayesian estimation approach is capable of handling a large set of yields. The involvement of these many yields also tends to improve the out-of-sample predictive accuracy of the yield curve forecasts. To show this, we also fit models with 4, 8, and 12 yields to data up to 2006. The last 4 quarters of 2007 are held aside for the validation of the predictions of the yields and the macro factors. These predictions are generated as described in Section 4.4. We measure the predictive accuracy of the forecasts in terms of the posterior predictive criterion (PPC) of Gelfand and Ghosh (1998). For a given model with λ number of the maturities, PPC is defined as

$$\text{PPC} = \text{D} + \text{W} \tag{4.1}$$

where

$$\text{D} = \frac{1}{\lambda + 2} \sum_{i=1}^{\lambda+2} \sum_{t=1}^T \text{Var}(\tilde{y}_{i,t} | \mathbf{y}, \mathcal{M}), \tag{4.2}$$

$$\text{W} = \frac{1}{\lambda + 2} \sum_{i=1}^{\lambda+2} \sum_{t=1}^T [y_{i,t} - E(\tilde{y}_{i,t} | \mathbf{y}, \mathcal{M})]^2 \tag{4.3}$$

$\{\tilde{\mathbf{y}}_t\}_{t=1,2,\dots,T}$ are the predictions of the yields and macro factors $\{\mathbf{y}_t\}_{t=1,2,\dots,T}$ under model \mathcal{M} , and $\tilde{y}_{i,t}$ and $y_{i,t}$ are the i th components of $\tilde{\mathbf{y}}_t$ and \mathbf{y}_t , respectively. The term D is expected to be large in models that are restrictive or have redundant parameters. The term W measures the predictive goodness-of-fit. As can be seen from Table 1, the model with 16 maturities outperforms the models with fewer maturities. The reason for this behavior is simple. The addition of a new yield introduces only one parameter (namely the pricing error variance) but because of the many cross-equation restrictions on the

The number of maturities(λ)	No change point model		
	D	W	PPC
4	6.293	4.821	11.114
8	5.827	4.758	10.585
12	4.621	4.191	8.812
16	4.011	3.520	7.531

Table 1: Posterior predictive criterion. *PPC is computed by 4.1 to 4.3. We use the data from the most recent break time point, 1995:II to 2006:IV due to the regime shift, and out of sample period is 2007:I-2007:IV. Four yields are of 2, 8, 20 and 40 quarters maturity bonds (used in Dai et al. (2007)). Eight yields are of 1, 2, 3, 4, 8, 12, 16 and 20 quarters maturity bonds(used in Bansal and Zhou (2002)). Twelve yields are of 1, 2, 3, 4, 5, 6, 8, 12, 20, 28, 32 and 40 quarters maturity bonds. Sixteen yields are of 1, 2, 3, 4, 5, 6, 7, 8, 10, 12, 16, 20, 24, 28, 32 and 40 quarters maturity bonds.*

parameters, the additional outcome helps to improve inferences about the common model parameters, which translates into improved predictive inferences.

4.1 Sampler Diagnostics

We base our results on 50,000 iterations of the MCMC algorithm beyond a burn-in of 5,000 iterations. We measure the efficiency of the MCMC sampling in terms of the metrics that are common in the Bayesian literature, in particular, the acceptance rates in the Metropolis-Hastings steps and the inefficiency factors (Chib (2001)) which, for any sampled sequence of draws, are defined as

$$1 + 2 \sum_{k=1}^K \rho(k), \quad (4.4)$$

where $\rho(k)$ is the k -order autocorrelation computed from the sampled variates and K is a large number which we choose conservatively to be 500. For our biggest model, the average acceptance rate and the average inefficiency factor in the M-H step are 72.9% and 174.1, respectively. These values indicate that our sampler mixes well. It is also important to mention that our sampler converges quickly to the same region of the parameter space regardless of the starting values.

4.2 The Number and Timing of Change Points

Table 2 contains the marginal likelihood estimates for our 5 contending models. As can be seen, the \mathcal{M}_3 is most supported by the data. We now provide more detailed results for this model.

Model	lnL	lnML	n.s.e.	$\Pr[\mathcal{M}_m \mathbf{y}]$	change point
\mathcal{M}_0	-1488.1	-1215.5	1.39	0.00	
\mathcal{M}_1	-1279.4	-955.5	1.77	0.00	1986:II
\mathcal{M}_2	-935.1	-665.4	1.92	0.00	1985:IV, 1995:II
\mathcal{M}_3	-473.4	-256.1	2.27	1.00	1980:II, 1985:IV, 1995:II
\mathcal{M}_4	-313.8	-281.4	2.62	0.00	1980:II, 1985:IV, 1995:II, 2002:III

Table 2: Log likelihood (lnL), log marginal likelihood (lnML), posterior probability of each model ($\Pr[\mathcal{M}_m|\mathbf{y}]$) under the assumption that the prior probability of each model is $1/5$, and change point estimates.

Our first set of findings relate to the timing of the change-points. Information about the change-points is gleaned from the sampled sequence of the states. Further details about how this is done can be obtained from Chib (1998). Of particular interest are the posterior probabilities of the timing of the regime changes. These probabilities are given in Figure 4. The figure reveals that the first 32 quarters (the first 8 years) belong to the first regime, the next 23 quarters (about 6 years) to the second, the next 38 quarters (about 9.5 years) to the third, and the remaining quarters to the fourth regime. Rudebusch and Wu (2007) also find a change point in the year of 1985. The finding of a break point in 1995 is striking as it has not been isolated from previous regime-change models.

We would like to emphasize that our estimates of the change points from the models without macro factors are exactly the same as those from the change point models with macro factors. We do not report those results in the interest of space. In addition, the results are not sensitive to our choice of 16 maturities, as we have confirmed.

4.3 Parameter Estimates

Table 3 summarizes the posterior distribution of the parameters. One point to note is that the posterior densities are generally different from the prior given in section 3.2,

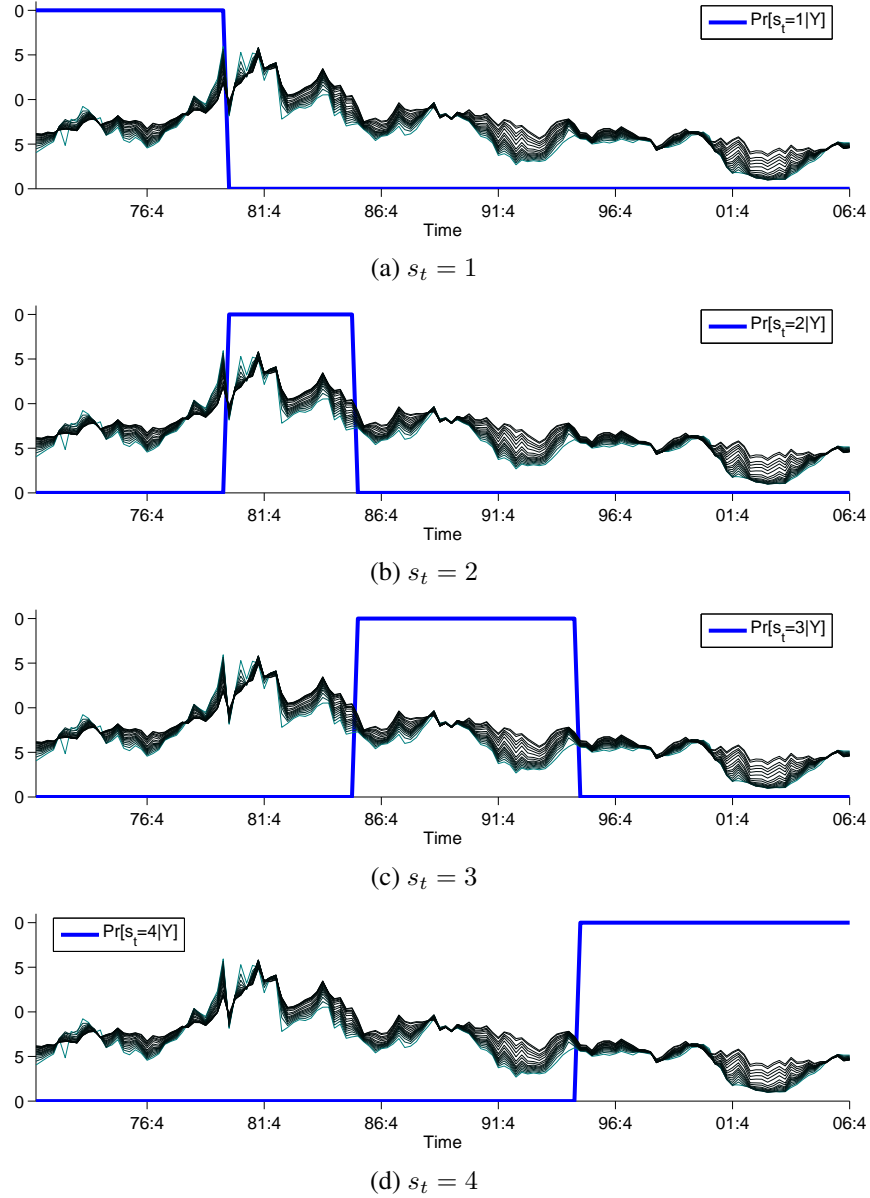


Figure 4: Model \mathcal{M}_3 : $\Pr(s_t = j | \mathbf{y})$. The posterior probabilities for each t are based on 50,000 MCMC draws of s_t - these probabilities are plotted along with the 16 yields in annualized percents (probabilities are multiplied by 20 for legibility).

which implies that the data is informative about these parameters. We focus on various aspects of this posterior distribution in the subsequent subsections.

	Regime 1			Regime 2			Regime 3			Regime 4		
G	0.90	0.07	0.15	0.95	-0.01	0.03	0.92	0.15	0.31	0.93	0.04	0.23
	(0.06)	(0.10)	(0.15)	(0.03)	(0.07)	(0.06)	(0.06)	(0.21)	(0.17)	(0.04)	(0.17)	(0.29)
	-0.24	0.67	-0.07	-0.07	0.73	-0.10	0.15	0.35	0.08	0.02	0.91	0.01
	(0.26)	(0.23)	(0.12)	(0.05)	(0.05)	(0.03)	(0.06)	(0.14)	(0.08)	(0.02)	(0.13)	(0.06)
	-0.06	-0.16	0.26	0.09	-0.35	0.52	-0.04	0.00	0.34	-0.03	-0.37	0.19
	(0.25)	(0.23)	(0.17)	(0.17)	(0.24)	(0.17)	(0.09)	(0.21)	(0.13)	(0.08)	(0.26)	(0.15)
μ $\times 400$	0.00	4.99	3.54	0.00	5.88	2.63	0.00	2.56	2.62	0.00	1.49	3.22
		(2.17)	(0.90)		(0.41)	(1.00)		(0.41)	(0.49)		(0.80)	(0.53)
	1.00			1.00			1.00			1.00		
L $\times 400$	0.11	1.72		0.10	1.48		0.11	0.74		-0.47	0.82	
	(0.40)	(0.19)		(0.44)	(0.13)		(0.34)	(0.13)		(0.59)	(0.12)	
	-0.67	-0.62	4.28	0.24	0.27	4.58	-0.55	-0.18	2.00	-0.13	-0.20	2.03
	(0.88)	(0.39)	(0.14)	(0.62)	(0.41)	(0.17)	(0.56)	(0.14)	(0.12)	(0.89)	(0.14)	(0.11)
δ_1 $\times 400$		9.23			2.78			4.42			4.34	
		(1.69)			(1.60)			(1.18)			(1.00)	
δ_2	1.16	0.09	0.17	1.29	0.25	0.16	0.72	0.31	0.26	0.57	0.56	0.10
	(0.13)	(0.23)	(0.22)	(0.16)	(0.23)	(0.15)	(0.09)	(0.26)	(0.21)	(0.07)	(0.37)	(0.25)
γ	-0.28	-0.40	-0.22	-0.34	-0.65	-0.21	-0.58	-0.56	-0.05	-0.34	-0.25	-0.19
	(0.28)	(0.30)	(0.26)	(0.25)	(0.21)	(0.26)	(0.28)	(0.33)	(0.24)	(0.25)	(0.25)	(0.27)
Φ	0.99	0.98	0.93	0.53	0.89	0.65	0.91	0.94	0.98	0.98	0.93	0.98
	(1.08)	(1.09)	(1.08)	(1.07)	(1.08)	(1.12)	(1.08)	(1.09)	(1.09)	(1.09)	(1.10)	(1.09)
p_{00}							0.934					
							(0.028)					
p_{11}							0.986					
							(0.004)					
p_{22}							0.987					
							(0.003)					

Table 3: Model \mathcal{M}_3 : Parameter estimates. *This table presents the posterior mean and standard deviation based on 50,000 MCMC draws beyond a burn-in of 5,000. The 95% credibility interval of parameters in bold face does not contain 0. Standard deviations are in parenthesis. The yields are of 1, 2, 3, 4, 5, 6, 7, 8, 10, 12, 16, 20, 24, 28, 36 and 40 quarters maturity bonds. Values without standard deviations are fixed by the identification restrictions.*

4.3.1 Factor Process

Figure 5 plots the average dynamics of the latent factors along with the short rate. This figure demonstrates that the latent factor movements are very close to those of the short rate. The estimates of the matrix \mathbf{G} for each regime show that the mean-reversion coefficient matrix is almost diagonal. The latent factor and inflation rate also display different degrees of persistence across regimes. In particular, the relative magnitudes of the diagonal elements indicates that the latent factor and the inflation factor are

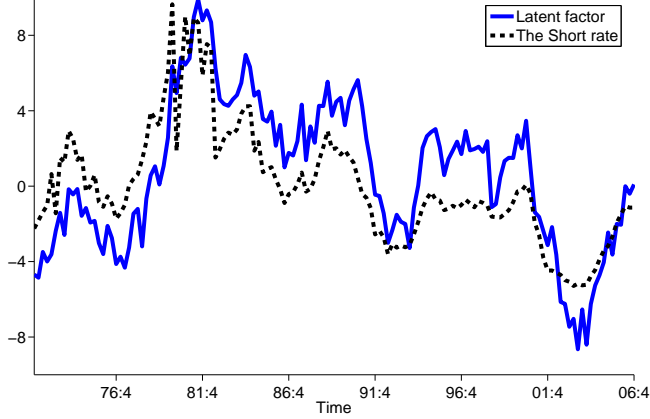


Figure 5: Model \mathcal{M}_3 : Estimates of the latent factor. *The short rate in percent is demeaned and estimates of the latent factor are calculated as the average of factor drawings given the 50,000 MCMC draws of the parameters.*

less mean-reverting in regime 2 and 4, respectively. For a more formal measure of this persistence, we calculate the eigenvalues of the coefficient matrices in each regime. These are given by

$$\begin{aligned} \text{eig}(\mathbf{G}_1) &= \begin{bmatrix} 0.851 \\ 0.709 \\ 0.267 \end{bmatrix}, & \text{eig}(\mathbf{G}_2) &= \begin{bmatrix} 0.978 \\ 0.814 \\ 0.401 \end{bmatrix} \\ \text{eig}(\mathbf{G}_3) &= \begin{bmatrix} 0.935 \\ 0.312 \\ 0.366 \end{bmatrix}, & \text{eig}(\mathbf{G}_4) &= \begin{bmatrix} 0.913 + 0.044i \\ 0.913 - 0.044i \\ 0.204 \end{bmatrix} \end{aligned}$$

It can be seen that the second regime has the largest absolute eigenvalue close to 1. Because the factor loadings for the latent factor ($\delta_{21,st}$) are significant whereas those for inflation ($\delta_{22,st}$) are not, the latent factor is responsible for most of the persistence of the yields.

Furthermore, the diagonal elements of \mathbf{L}_3 and \mathbf{L}_4 are even smaller than their counterparts in \mathbf{L}_1 and \mathbf{L}_2 . This suggests a reduction in factor volatility starting from the middle of the 1980s, which coincides with the period that is called the great moderation (Kim, Nelson, and Piger (2004)).

4.3.2 Factor Loadings

The factor loadings in the short rate equation, δ_{2,s_t} are all positive, which is consistent with the conventional wisdom that central bankers tend to raise the interest rate in response to a positive shock to the macro factors. It can also be seen that δ_{2,s_t} along with \mathbf{G}_{s_t} and \mathbf{L}_{s_t} are different across regimes, which makes the factor loadings regime-dependent across the term structure as revealed in figure 6. This finding lends support to our assumption of regime-dependent factor loadings.

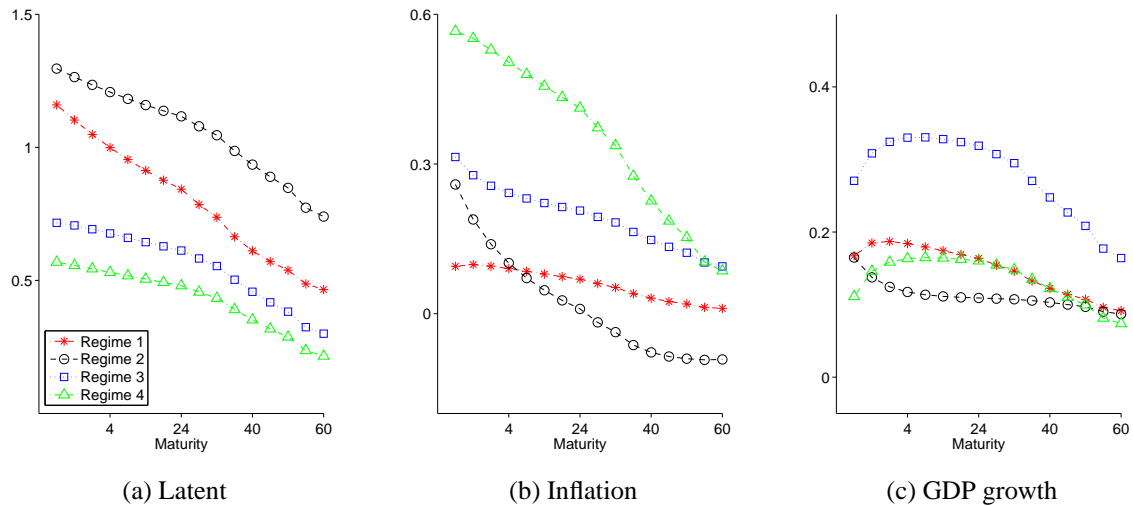


Figure 6: Model \mathcal{M}_3 : Estimates of the factor loadings, $\bar{\mathbf{b}}_{s_t}$. The factor loadings represent the average simulated factor loadings from the retained 50,000 MCMC iterations.

4.3.3 Term Premium

Figure 7 plots the posterior distribution of the term premium of the two year maturity bond over time. It is interesting to observe how the term premium varies across regimes. In particular, the term premium is the lowest in the most recent regime (although the .025 quantile of the term premium distribution in the first regime is lower than the .025 quantile of term premium distribution in the most current regime). This can be attributed to the lower value of factor volatilities in this regime. Moreover, we find that these changes in the term premium are not closely related to changes in the latent and macro-economic factors. A similar finding appears in Rudebusch, Sack, and Swanson (2007).

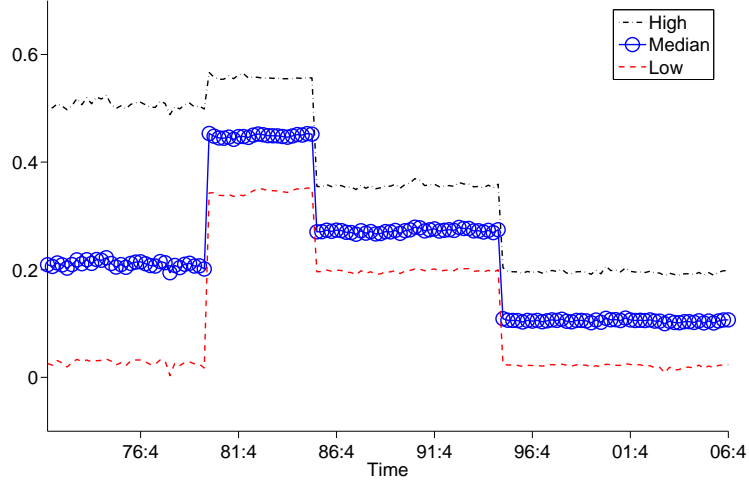


Figure 7: Model \mathcal{M}_3 : Term premium. The figure plots the 2.5%, 50% and 97.5% quantile of the posterior term premium based on 50,000 MCMC draws beyond a burn-in of 5,000 iterations.

4.3.4 Pricing Error Volatility

In Figure 8 we plot the term structure of the pricing error standard deviations. As in the no-change point model of Chib and Ergashev (2009), these are hump-shaped in each regime. One can also see that these standard deviations have changed over time, primarily for the short-bonds. These changes in the volatility also help to determine the timing of the change-points.

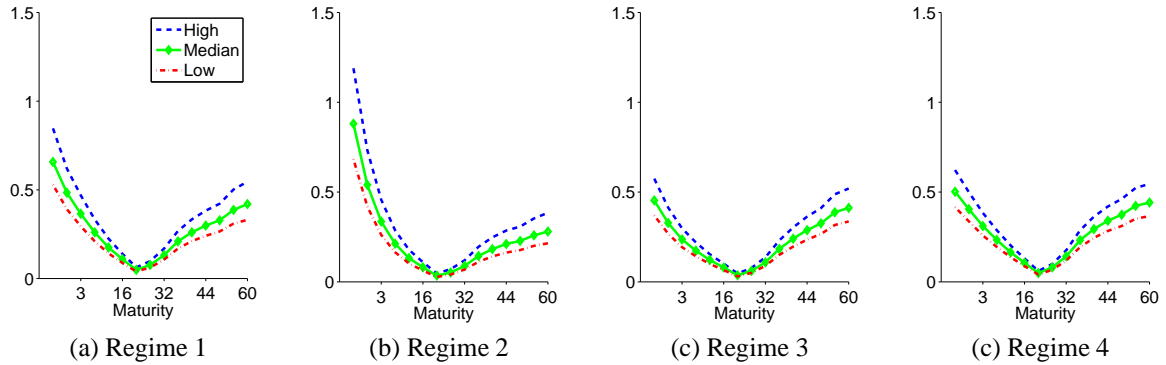


Figure 8: Model \mathcal{M}_3 : Term Structure of the Pricing Error Volatility. The figures display the 2.5%, 50% and 97.5% quantile of the posterior standard deviation of the pricing errors.

4.4 Forecasting and Predictive Densities

A principle objective of this paper is to compare the forecasting abilities of the affine term structure models with and without regime changes. In the Bayesian paradigm, it is relatively straightforward to simulate the predictive density from the MCMC output. By definition, the predictive density of the future observations, conditional on the data, is the integral of the density of the future outcomes given the the parameters with respect to the posterior distribution of the parameters. If we let \mathbf{y}_f denote the future observations, the predictive density under model \mathcal{M}_m is given by

$$p(\mathbf{y}_f|\mathcal{M}_m, \mathbf{y}) = \int_{\boldsymbol{\psi}} p(\mathbf{y}_f|\mathcal{M}_m, \mathbf{y}, \boldsymbol{\psi})\pi(\boldsymbol{\psi}|\mathcal{M}_m, \mathbf{y})d\boldsymbol{\psi} \quad (4.5)$$

This density can be sampled by the method of composition as follows. For each MCMC iteration (beyond the burn-in period), conditioned on \mathbf{f}_n and the parameters in the current terminal regime (which is not necessarily regime $m + 1$), we draw the factors \mathbf{f}_{n+1} based on the equation (2.3). Then given \mathbf{f}_{n+1} , the yields \mathbf{R}_{n+1} are drawn using equation (3.8). These two steps are iterated forward to produce the draws \mathbf{f}_{n+i} and \mathbf{R}_{n+i} , $i = 1, 2, \dots, T$. Repeated over the course of the MCMC iterations, these steps produce a collection of simulated macro factors and yields that is a sample from the predictive density.

We summarize the sampled predictive densities in Figure 9. The top panel gives the forecast intervals from the \mathcal{M}_0 model and the bottom panel has the forecast intervals from the \mathcal{M}_3 model. Note that in both cases the actual yield curve in each of the four quarters of 2007 is bracketed by the corresponding 95% credibility interval though the intervals from the \mathcal{M}_3 model are tighter.

For a more formal forecasting performance comparison, we tabulate the PPC for each case in Table 4. We also include in the last column of this table an interesting set of results that make use of the regimes isolated by our \mathcal{M}_3 model. In particular, we fit the no-change point model to the data in the last regime but ending just before our different forecast periods (2005:I-2005:IV, 2006:I-2006:IV and 2007:I-2007:IV). As one would expect, the forecasts from the no-change point model estimated on the sample period of the last regime are similar to those from the \mathcal{M}_3 model. Thus, given the regimes we have isolated, a poor-man's approach to forecasting the term-structure would be to

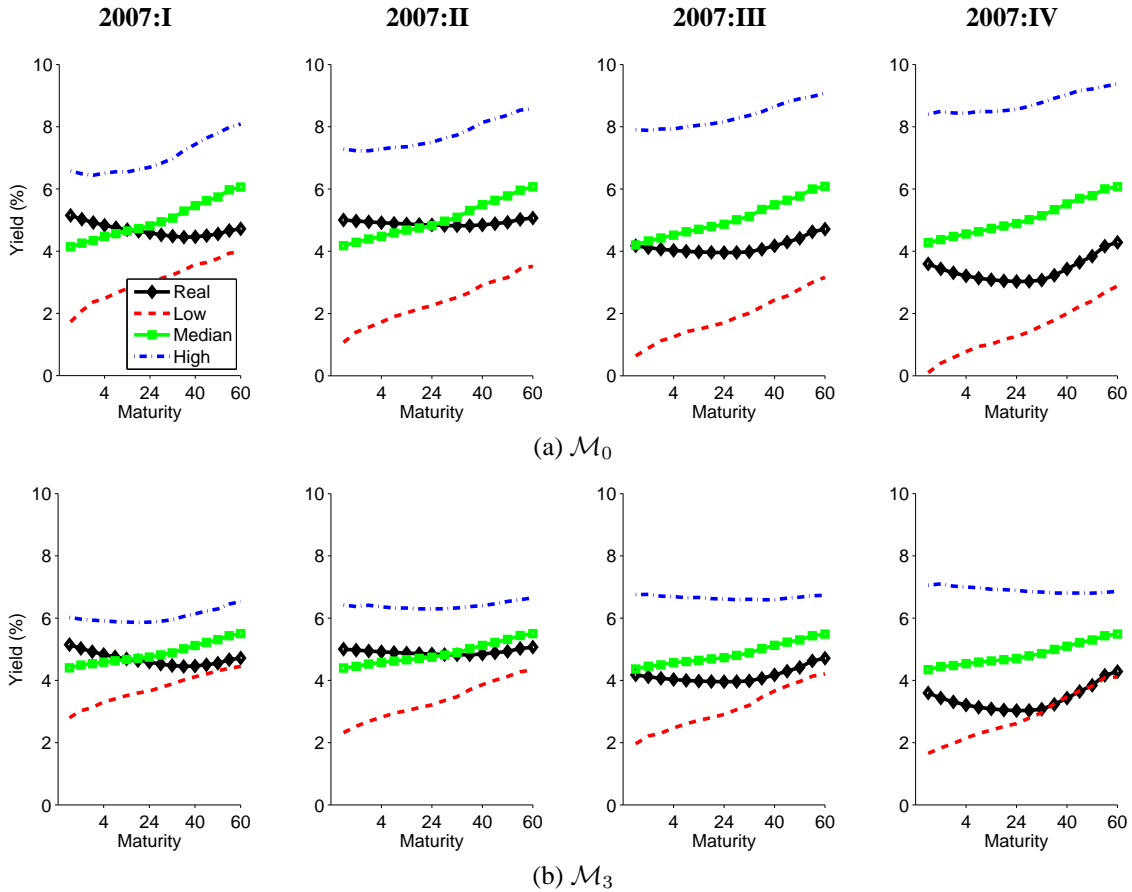


Figure 9: Predicted yield curve. *The figures present four quarters ahead forecasts of the yields on the T-bills. The top panel is based on the no change point model and the bottom panel on the three change point model. In each case, the 2.5%, 50% and 97.5% quantile curves are based on 50,000 forecasted values for the period 2007:I-2007:IV. The observed curves are labeled “Real”.*

fit the no-change arbitrage-free yield model to the last regime. Of course, the predictions from the \mathcal{M}_3 model produce a smaller value of the PPC than those from the no-change point model that is fit to the whole sample. This, combined with the in-sample fit of the models as measured by the marginal likelihoods, suggests that the change point model outperforms the no-change point version. These findings not only reaffirm the finding of structural changes, but also suggest that there are gains to incorporating regime changes when forecasting the term structure of interest rates.

model	\mathcal{M}_0	\mathcal{M}_1	\mathcal{M}_2	\mathcal{M}_3	\mathcal{M}_4	\mathcal{M}_0
sample period	(1972:I-2006:IV)					(1995:II-2006:IV)
D	12.548	5.401	4.156	4.720	4.599	4.011
W	5.678	4.896	4.201	3.415	2.902	3.520
PPC	18.226	10.297	8.357	8.126	7.501	7.531

(a) *forecast period: 2007:I-2007:IV*

model	\mathcal{M}_0	\mathcal{M}_1	\mathcal{M}_2	\mathcal{M}_3	\mathcal{M}_4	\mathcal{M}_0
sample period	(1972:I-2005:IV)					(1995:II-2005:IV)
D	12.606	5.799	4.157	4.097	7.011	4.271
W	2.137	5.658	4.432	1.817	3.036	2.390
PPC	14.743	11.457	8.589	5.914	10.047	6.661

(b) *forecast period: 2006:I-2006:IV*

model	\mathcal{M}_0	\mathcal{M}_1	\mathcal{M}_2	\mathcal{M}_3	\mathcal{M}_4	\mathcal{M}_0
sample period	(1972:I-2004:IV)					(1995:II-2004:IV)
D	13.474	5.187	3.572	4.609	7.190	3.919
W	2.367	5.787	4.442	1.977	2.657	2.359
PPC	15.841	10.974	8.014	6.587	9.847	6.278

(c) *forecast period: 2005:I-2005:IV*

Table 4: Posterior predictive criterion. PPC is computed by (4.1) to (4.3).

5 Concluding Remarks

In this paper we have developed a new model of the term structure of zero-coupon bonds with regime changes. This paper complements the recent developments in this area because it is organized around a different model of regime changes than the Markov switching model that has been used to date. It also complements the recent work on affine models with macro factors which has been done in settings without regime changes. The models we fit involve more bonds than has ever been attempted in the literature. This in turn leads to a better fit to the data. Furthermore, we incorporate some recent developments in Bayesian econometrics that make it possible to estimate the large scale models in this paper.

Our empirical analysis suggests that the term structure has gone through three change points, and that the term structure and the risk premium are materially different across regimes. Our analysis also shows that there are gains in predictive accuracy by incorporating regime changes when forecasting the term structure of interest rates.

A Bond Prices under Regime Changes

By the assumption of the affine model, we have

$$P_t(s_t, \tau) = \exp(-a_{s_t}(\tau) - \mathbf{b}_{s_t}(\tau)'(\mathbf{f}_t - \boldsymbol{\mu}_{s_t})) \quad (\text{A.1})$$

$$\text{and } P_{t+1}(s_{t+1}, \tau - 1) = \exp(-a_{s_{t+1}}(\tau - 1) - \mathbf{b}_{s_{t+1}}(\tau - 1)'(\mathbf{f}_{t+1} - \boldsymbol{\mu}_{s_{t+1}})).$$

Let $h_{\tau, t+1}$ denote

$$\frac{P_{t+1}(s_{t+1}, \tau - 1)}{P_t(s_t, \tau)} = \exp[-a_{s_{t+1}}(\tau - 1) - \mathbf{b}_{s_{t+1}}(\tau - 1)'(\mathbf{f}_{t+1} - \boldsymbol{\mu}_{s_{t+1}}) + a_{s_t}(\tau) + \mathbf{b}_{s_t}(\tau)'(\mathbf{f}_t - \boldsymbol{\mu}_{s_t})] \quad (\text{A.2})$$

It immediately follows from the bond pricing formula that

$$\begin{aligned} 1 &= \mathbf{E}_t \left[\kappa_{t, s_t, t+1} \frac{P_{t+1}(s_{t+1}, \tau - 1)}{P_t(s_t, \tau)} \right] \\ &= \mathbf{E}_t [\kappa_{t, s_t, t+1} h_{\tau, t+1}]. \end{aligned} \quad (\text{A.3})$$

Then by substitution

$$\begin{aligned} &\kappa_{t, s_t, t+1} h_{\tau, t+1} \quad (\text{A.4}) \\ &= \exp[-r_{t, s_t} - \frac{1}{2} \boldsymbol{\gamma}'_{t, s_t} \boldsymbol{\gamma}_{t, s_t} - \boldsymbol{\gamma}'_{t, s_t} \mathbf{L}_{s_{t+1}}^{-1} \boldsymbol{\eta}_{t+1} \\ &\quad - a_{s_{t+1}}(\tau - 1) - \mathbf{b}_{s_{t+1}}(\tau - 1)'(\mathbf{f}_{t+1} - \boldsymbol{\mu}_{s_{t+1}}) + a_{s_t}(\tau) + \mathbf{b}_{s_t}(\tau)'(\mathbf{f}_t - \boldsymbol{\mu}_{s_t})] \\ &= \exp[-R_{t, s_t} - \frac{1}{2} \boldsymbol{\gamma}'_{t, s_t} \boldsymbol{\gamma}_{t, s_t} - (\boldsymbol{\gamma}'_{t, s_t} \mathbf{L}_{s_{t+1}}^{-1} + \mathbf{b}_{s_{t+1}}(\tau - 1)') \boldsymbol{\eta}_{t+1} + \zeta_{\tau, s_t, s_{t+1}}] \\ &= \exp[-R_{t, s_t} - \frac{1}{2} \boldsymbol{\gamma}'_{t, s_t} \boldsymbol{\gamma}_{t, s_t} - (\boldsymbol{\gamma}_{t, s_t} + \mathbf{b}_{s_{t+1}}(\tau - 1)' \mathbf{L}_{s_{t+1}}) \boldsymbol{\omega}_{t+1} + \zeta_{\tau, s_t, s_{t+1}}] \\ &= \exp[-R_{t, s_t} - \frac{1}{2} \boldsymbol{\gamma}'_{t, s_t} \boldsymbol{\gamma}_{t, s_t} + \frac{1}{2} \boldsymbol{\Gamma}_{t, \tau} \boldsymbol{\Gamma}'_{t, \tau} + \zeta_{\tau, s_t, s_{t+1}}] \exp[-\frac{1}{2} \boldsymbol{\Gamma}_{t, \tau} \boldsymbol{\Gamma}'_{t, \tau} - \boldsymbol{\Gamma}_{t, \tau} \boldsymbol{\omega}_{t+1}] \end{aligned}$$

where

$$\begin{aligned} \zeta_{\tau, s_t, s_{t+1}} &= a_{s_t}(\tau) + \mathbf{b}_{s_t}(\tau)'(\mathbf{f}_t - \boldsymbol{\mu}_{s_t}) - a_{s_{t+1}}(\tau - 1) - \mathbf{b}_{s_{t+1}}(\tau - 1)' \mathbf{G}_{s_{t+1}}(\mathbf{f}_t - \boldsymbol{\mu}_{s_t}) \\ \boldsymbol{\Gamma}_{t, \tau} &= \boldsymbol{\gamma}'_{t, s_t} + \mathbf{b}_{s_{t+1}}(\tau - 1)' \mathbf{L}_{s_{t+1}} \end{aligned}$$

and $\boldsymbol{\omega}_{t+1} = \mathbf{L}_{s_{t+1}}^{-1} \boldsymbol{\eta}_{t+1} \sim \mathcal{N}(0, \mathbf{I}_{k+m})$. Given \mathbf{f}_t, s_{t+1} and s_t , the only random variable in $\kappa_{t, t+1} h_{\tau, t+1}$ is $\boldsymbol{\omega}_{t+1}$. Then since

$$\mathbf{E}_t \left(\exp[-\frac{1}{2} \boldsymbol{\Gamma}_{t, \tau} \boldsymbol{\Gamma}'_{t, \tau} - \boldsymbol{\Gamma}_{t, \tau} \boldsymbol{\omega}_{t+1}] \right) = 1 \quad (\text{A.5})$$

we have that

$$\mathbf{E} [\kappa_{t,s_t,t+1} h_{\tau,t+1} | \mathbf{f}_t, s_{t+1}, s_t] = \exp[-R_{t,s_t} - \frac{1}{2} \gamma'_{t,s_t} \gamma_{t,s_t} + \frac{1}{2} \Gamma_{t,\tau} \Gamma'_{t,\tau} + \zeta_{\tau,s_t,s_{t+1}}].$$

Using log-approximation $\exp(y) \approx y + 1$ for a sufficiently small y leads to

$$\begin{aligned} & \mathbf{E} [\kappa_{t,s_t,t+1} h_{\tau,t+1} | \mathbf{f}_t, s_{t+1}, s_t] & (A.6) \\ &= \exp[-R_{t,s_t} - \frac{1}{2} \gamma'_{t,s_t} \gamma_{t,s_t} + \frac{1}{2} (\gamma'_{t,s_t} + \mathbf{b}_{s_{t+1}}(\tau - 1)' \mathbf{L}_{s_{t+1}}) (\gamma_{t,s_t} + \mathbf{b}_{s_{t+1}}(\tau - 1)' \mathbf{L}_{s_{t+1}})' + \zeta_{\tau,s_t,s_{t+1}}] \\ &\approx -R_{t,s_t} + \gamma'_{t,s_t} \mathbf{L}'_{s_{t+1}} \mathbf{b}_{s_{t+1}}(\tau - 1) + \frac{1}{2} (\mathbf{b}_{s_{t+1}}(\tau - 1)' \mathbf{L}_{s_{t+1}} \mathbf{L}'_{s_{t+1}} \mathbf{b}_{s_{t+1}}(\tau - 1)) + \zeta_{\tau,s_t,s_{t+1}} + 1 \\ &= -(\delta_{1,s_t} + \delta'_{2,s_t} (\mathbf{f}_t - \boldsymbol{\mu}_{s_t})) + (\tilde{\gamma}_{s_t} + \Phi_{s_t} (\mathbf{f}_t - \boldsymbol{\mu}_{s_t}))' \mathbf{L}'_{s_{t+1}} \mathbf{b}_{s_{t+1}}(\tau - 1) \\ &+ \frac{1}{2} (\mathbf{b}_{s_{t+1}}(\tau - 1)' \mathbf{L}_{s_{t+1}} \mathbf{L}'_{s_{t+1}} \mathbf{b}_{s_{t+1}}(\tau - 1)) + \zeta_{\tau,s_t,s_{t+1}} + 1 \end{aligned}$$

Given the information at time t , (i.e. \mathbf{f}_t and $s_t = j$), integrating out s_{t+1} yields

$$\begin{aligned} \mathbf{E} [\kappa_{t,s_t,t+1} h_{\tau,t+1} | \mathbf{f}_t, s_t = j] &= \sum_{s_{t+1}=j,k} p_{js_{t+1}} \mathbf{E} [\kappa_{t,s_t,t+1} h_{\tau,t+1} | \mathbf{f}_t, s_{t+1}, s_t = j] & (A.7) \\ &= 1 \text{ where } k = j + 1. \end{aligned}$$

Thus we have

$$\begin{aligned} 0 &= \sum_{s_{t+1}=j,k} p_{js_{t+1}} \{ \mathbf{E} [\kappa_{t,s_t,t+1} h_{\tau,t+1} | \mathbf{f}_t, s_{t+1}, s_t = j] - 1 \} \text{ since } \sum_{s_{t+1}=j,k} p_{js_{t+1}} = 1 & (A.8) \\ &= p_{jj} (\mathbf{E} [\kappa_{t,s_t,t+1} h_{\tau,t+1} | \mathbf{f}_t, s_{t+1} = j, s_t = j] - 1) + p_{jk} (\mathbf{E} [\kappa_{t,s_t,t+1} h_{\tau,t+1} | \mathbf{f}_t, s_{t+1} = k, s_t = j] - 1) \\ &\approx -p_{jj} (\delta_{1,j} + \delta'_{2,j} (\mathbf{f}_t - \boldsymbol{\mu}_{s_t})) + p_{jj} (\tilde{\gamma}_j + \Phi_j (\mathbf{f}_t - \boldsymbol{\mu}_{s_t}))' \mathbf{L}'_j \mathbf{b}_j(\tau - 1) \\ &+ \frac{1}{2} p_{jj} (\mathbf{b}_j(\tau - 1)' \mathbf{L}_j \mathbf{L}'_j \mathbf{b}_j(\tau - 1)) + p_{jj} \zeta_{\tau,j,j} \\ &- p_{jk} (\delta_{1,j} + \delta'_{2,j} (\mathbf{f}_t - \boldsymbol{\mu}_{s_t})) + p_{jk} (\tilde{\gamma}_j + \Phi_j (\mathbf{f}_t - \boldsymbol{\mu}_{s_t}))' \mathbf{L}'_k \mathbf{b}_k(\tau - 1) \\ &+ \frac{1}{2} p_{jk} (\mathbf{b}_k(\tau - 1)' \mathbf{L}_k \mathbf{L}'_k \mathbf{b}_k(\tau - 1)) + p_{jk} \zeta_{\tau,j,k} \end{aligned}$$

Matching the coefficients on \mathbf{f}_t and setting the constant terms equal to zero we obtain the recursive equation for $a_{s_t}(\tau)$ and $\mathbf{b}_{s_t}(\tau)$ given the initial conditions $a_{s_t}(0) = 0$ and $\mathbf{b}_{s_t}(0) = \mathbf{0}_{3 \times 1}$ implied by the no-arbitrage condition. Finally imposing the restrictions on the transition probabilities establishes the proof.

B MCMC Sampling

This section provides the details of the MCMC algorithm given in section 3.4. The algorithm is coded in Gauss 9.0 and executed on a Windows Vista 62-bit machine with

a 2.66 GHz Intel Quad Core2 CPU. About 12 days are needed to generate 50,000 MCMC draws in the 3 change-point model. In contrast, a random-walk M-H algorithm takes about 2 days to complete 1 million iterations but with unknown reliability and much less efficient exploration (Chib and Ramamurthy (2009)).

Step 2 Sampling θ

We sample θ conditioned on $(\mathbf{S}_n, u_0, \sigma^{*2})$ by the tailored randomized block M-H (TaRB-MH) algorithm introduced in Chib and Ramamurthy (2009). The schematics of the TaRB-MH algorithm are as follows. The parameters in θ are first randomly partitioned into various sub-blocks at the beginning of an iteration. Each of these sub-blocks is then sampled in sequence by drawing a value from a tailored proposal density constructed for that particular block; this proposal is then accepted or rejected by the usual M-H probability of move (Chib and Greenberg (1995)). For instance, suppose that in the g th iteration, we have h_g sub-blocks of θ

$$\theta_1, \theta_2, \dots, \theta_{h_g}$$

If ψ_{-i} denotes the collection of the parameters in ψ except θ_i , then the proposal density $q(\theta_i | \mathbf{y}, \psi_{-i})$ for the i th block conditioned on ψ_{-i} is constructed by a quadratic approximation at the mode of the current target density $\pi(\theta_i | \mathbf{y}, \psi_{-i})$. In our case, we let this proposal density take the form of a student t distribution with 15 degrees of freedom

$$q(\theta_i | \mathbf{y}, \psi_{-i}) = St\left(\theta_i | \hat{\theta}_i, \mathbf{V}_{\hat{\theta}_i}, 15\right) \quad (\text{B.1})$$

where

$$\begin{aligned} \hat{\theta}_i &= \arg \max_{\theta_i} \ln\{p(\mathbf{y} | \mathbf{S}_n, \theta_i, \psi_{-i})\pi(\theta_i)\} \\ \text{and } \mathbf{V}_{\hat{\theta}_i} &= \left(-\frac{\partial^2 \ln\{p(\mathbf{y} | \mathbf{S}_n, \theta_i, \psi_{-i})\pi(\theta_i)\}}{\partial \theta_i \partial \theta_i'} \right)_{|\theta_i = \hat{\theta}_i}^{-1}. \end{aligned} \quad (\text{B.2})$$

Because the likelihood function tends to be ill-behaved in these problems, we calculate $\hat{\theta}_i$ using a suitably designed version of the simulated annealing algorithm. In our experience, this stochastic optimization method works better than the standard Newton-Raphson class of deterministic optimizers.

We then generate a proposal value $\boldsymbol{\theta}_i^\dagger$ which, upon satisfying all the constraints, is accepted as the next value in the chain with probability

$$\begin{aligned} & \alpha(\boldsymbol{\theta}_i^{(g-1)}, \boldsymbol{\theta}_i^\dagger | \mathbf{y}, \boldsymbol{\psi}_{-i}) \\ &= \min \left\{ \frac{p(\mathbf{y} | \mathbf{S}_n, \boldsymbol{\theta}_i^\dagger, \boldsymbol{\psi}_{-i}) \pi(\boldsymbol{\theta}_i^\dagger)}{p(\mathbf{y} | \mathbf{S}_n, \boldsymbol{\theta}_i^{(g-1)}, \boldsymbol{\psi}_{-i}) \pi(\boldsymbol{\theta}_i^{(g-1)})} \frac{St(\boldsymbol{\theta}_i^{(g-1)} | \hat{\boldsymbol{\theta}}_i, \mathbf{V}_{\hat{\boldsymbol{\theta}}_i}, 15)}{St(\boldsymbol{\theta}_i^\dagger | \hat{\boldsymbol{\theta}}_i, \mathbf{V}_{\hat{\boldsymbol{\theta}}_i}, 15)}, 1 \right\}. \end{aligned} \quad (\text{B.3})$$

If $\boldsymbol{\theta}_i^\dagger$ violates any of the constraints in \mathcal{R} , it is immediately rejected. The simulation of $\boldsymbol{\theta}$ is complete when all the sub-blocks

$$\pi(\boldsymbol{\theta}_1 | \mathbf{y}, \mathbf{S}_n, \boldsymbol{\psi}_{-1}), \pi(\boldsymbol{\theta}_2 | \mathbf{y}, \mathbf{S}_n, \boldsymbol{\psi}_{-2}), \dots, \pi(\boldsymbol{\theta}_{h_g} | \mathbf{y}, \mathbf{S}_n, \boldsymbol{\psi}_{-h_g}) \quad (\text{B.4})$$

are sequentially updated as above.

Step 3 Sampling the initial factor

Given the prior in equation (3.14), u_0 is updated conditioned on $\boldsymbol{\theta}$, \mathbf{m}_0 and $\mathbf{f}_1 = (u_1 \mathbf{m}'_1)'$, where \mathbf{m}_0 is given by data and u_1 is obtained from the equation (3.5). In the following, it is assumed that all the underlying coefficients are those in regime 0. Then

$$u_0 | \mathbf{f}_1, \boldsymbol{\theta} \sim \mathcal{N}_1(\bar{u}_0, \mathbf{U}_0) \quad (\text{B.5})$$

where

$$\bar{u}_0 = \mathbf{U}_0 (\boldsymbol{\Sigma}_u^{-1} + \mathbf{H}^* \boldsymbol{\Omega}_{11,0}^* u_1^*), \quad \mathbf{U}_0 = (\boldsymbol{\Sigma}_u^{-1} + \mathbf{H}^* \boldsymbol{\Omega}_{11,1}^* \mathbf{H}^*)$$

and on letting

$$\begin{aligned} \mathbf{G}_0 &= \begin{pmatrix} \mathbf{G}_{11,1} & \mathbf{G}_{12,1} \\ \mathbf{G}_{21,1} & \mathbf{G}_{22,1} \end{pmatrix}, \quad \boldsymbol{\Omega}_1 = \begin{pmatrix} \Omega_{11,1} & \Omega_{12,1} \\ \Omega_{21,1} & \Omega_{22,1} \end{pmatrix} \\ \mathbf{H}^* &= \mathbf{G}_{11,1} - \Omega_{12,1} \Omega_{22,1}^{-1} \mathbf{G}_{21,1}, \quad \boldsymbol{\Omega}_{11,1}^* = \Omega_{11,1} - \Omega_{12,1} \Omega_{22,1}^{-1} \Omega_{21,1} \\ u_1^* &= u_1 - \Omega_{12,1} \Omega_{22,1}^{-1} (\mathbf{m}_1 - \boldsymbol{\mu}_{m,1}) + (\Omega_{12,1} \Omega_{22,1}^{-1} \mathbf{G}_{22,1} - \mathbf{G}_{12,1}) (\mathbf{m}_0 - \boldsymbol{\mu}_{m,1}) \end{aligned}$$

Step 4 Sampling regimes

In this step one samples the states from $p[\mathbf{S}_n | I_n, \boldsymbol{\psi}]$ where I_n is the history of the outcomes up to time n . This is done according to the method of Chib (1996) and Chib (1998) by sampling \mathbf{S}_n in a single block from the output of one forward and backward pass through the data.

The forward recursion is initialized at $t = 1$ by setting $\Pr[s_1 = 1|I_1, \boldsymbol{\psi}] = 1$. Then one first obtains $\Pr[s_t = j|I_t, \boldsymbol{\psi}]$ for all $j = 1, 2, \dots, m + 1$ and $t = 1, 2, \dots, n$ by calculating

$$\Pr[s_t = j|I_t, \boldsymbol{\psi}] = \sum_{i=j-1}^j \Pr[s_{t-1} = i, s_t = j|I_t, \boldsymbol{\psi}] \quad (\text{B.6})$$

where

$$\Pr[s_{t-1} = i, s_t = j|I_t, \boldsymbol{\psi}] = \frac{p[\mathbf{y}_t|I_{t-1}, s_{t-1} = i, s_t = j, \boldsymbol{\psi}] \Pr[s_{t-1} = i, s_t = j|I_{t-1}, \boldsymbol{\psi}]}{p[\mathbf{y}_t|I_{t-1}, \boldsymbol{\psi}]}$$

This can be done by the equations (3.22)-(3.25).

In the backward pass, one simulates \mathbf{S}_n by the method of composition. One samples s_n from $\Pr[s_n = 1|I_n, \boldsymbol{\psi}]$. We remark that in this sampling step, s_n can take any value in $\{1, 2, \dots, m + 1\}$. For instance, if s_n turns out to be m and not $(m + 1)$, then m is taken to be the absorbing regime and the parameters of regime $(m + 1)$ are drawn from the prior in that iteration. In our data, however, $(m + 1)$ is always drawn because the last change point occurs in the interior of the sample and, therefore, the distribution $\Pr[s_n = 1|I_n, \boldsymbol{\psi}]$ has almost a unit mass on $(m + 1)$. Then for $t = 1, 2, \dots, n - 1$ we sequentially calculate

$$\begin{aligned} \Pr[s_t = j|I_t, s_{t+1} = k, S^{t+2}, \boldsymbol{\psi}] &= \Pr[s_t = j|I_t, s_{t+1} = k, \boldsymbol{\psi}] \quad (\text{B.7}) \\ &= \frac{\Pr[s_{t+1} = k|s_t = j] \Pr[s_t = j|I_t, \boldsymbol{\psi}]}{\sum_{j=k-1}^k \Pr[s_{t+1} = k|s_t = j] \Pr[s_t = j|I_t, \boldsymbol{\psi}]} \end{aligned}$$

where $S^{t+1} = \{s_{t+1}, \dots, s_n\}$ denotes the set of simulated states from the earlier steps. A value s_t is drawn from this distribution and it is either the value k or $(k - 1)$ conditioned on $s_{t+1} = k$.

Step 5 Sampling the variances of the pricing errors

A convenient feature of our modeling approach is that, conditional on the history of the regimes and factors, the joint distribution of the parameters in $\boldsymbol{\sigma}^{*2}$ is analytically tractable and takes the form of an inverse gamma density. Thus, for $i \in \{1, 2, \dots, 7, 9, \dots, 16\}$ and $j = 1, 2, \dots, m + 1$, $\sigma_{i,j}^{*2}$ is sampled from

$$\text{IG} \left\{ \frac{\bar{v} + \sum_{t=1}^n I(s_t = j)}{2}, \frac{\bar{d} + \sum_{t=1}^n d_{i,j} I(s_t = j) (R_{it} - \bar{a}_{i,j} - \bar{\mathbf{b}}'_{i,j} (\mathbf{f}_t - \boldsymbol{\mu}_j))^2}{2} \right\} \quad (\text{B.8})$$

where $I(\cdot)$ is the indicator function.

References

- Ang, A., Bekaert, G., and Wei, M. (2008), “The term structure of real rates and expected inflation,” *Journal of Finance*, 63, 797–849.
- Ang, A., Dong, S., and Piazzesi, M. (2007), “No-arbitrage Taylor rules,” *Columbia University working paper*.
- Ang, A. and Piazzesi, M. (2003), “A no-arbitrage vector autoregression of term structure dynamics with macroeconomic and latent variables,” *Journal of Monetary Economics*, 50, 745–787.
- Bansal, R. and Zhou, H. (2002), “Term structure of interest rates with regime shifts,” *Journal of Finance*, LVII, 463–473.
- Chen, R. and Scott, L. (2003), “ML estimation for a multifactor equilibrium model of the term structure,” *Journal of Fixed Income*, 27, 14–31.
- Chib, S. (1995), “Marginal likelihood from the Gibbs output,” *Journal of the American Statistical Association*, 90, 1313–1321.
- (1996), “Calculating posterior distributions and modal estimates in Markov mixture models,” *Journal of Econometrics*, 75, 79–97.
- (1998), “Estimation and comparison of multiple change-point models,” *Journal of Econometrics*, 86, 221–241.
- (2001), “Markov chain Monte Carlo methods: computation and inference,” in *Handbook of Econometrics*, eds. Heckman, J. and Leamer, E., North Holland, Amsterdam, vol. 5, pp. 3569–3649.
- Chib, S. and Ergashev, B. (2009), “Analysis of multi-factor affine yield curve models,” *Journal of the American Statistical Association*, forthcoming.
- Chib, S. and Greenberg, E. (1995), “Understanding the Metropolis-Hastings algorithm,” *American Statistician*, 49, 327–335.

- Chib, S. and Jeliazkov, I. (2001), “Marginal likelihood from the Metropolis-Hastings output,” *Journal of the American Statistical Association*, 96, 270–281.
- Chib, S. and Ramamurthy, S. (2009), “Tailored randomized block MCMC methods with application to DSGE models,” *Journal of Econometrics*, forthcoming.
- Dai, Q. and Singleton, K. J. (2000), “Specification analysis of affine term structure models,” *Journal of Finance*, 55, 1943–1978.
- Dai, Q., Singleton, K. J., and Yang, W. (2007), “Regime shifts in a dynamic term structure model of U.S. treasury bond yields,” *Review of Financial Studies*, 20, 1669–1706.
- Duffie, G. and Kan, R. (1996), “A yield-factor model of interest rates,” *Mathematical Finance*, 6, 379–406.
- Gelfand, A. E. and Ghosh, S. K. (1998), “Model choice: A minimum posterior predictive loss approach,” *Biometrika*, 85, 1–11.
- Gurkaynak, R. S., Sack, B., and Wright, J. H. (2007), “The U.S. treasury yield curve: 1961 to the present,” *Journal of Monetary Economics*, 54, 2291–2304.
- Kim, C. J., Nelson, C. R., and Piger, J. (2004), “The less volatile U.S. economy: a Bayesian investigation of timing, breadth, and potential explanations,” *Journal of Business and Economic Statistics*, 22, 80–93.
- Rudebusch, G. D., Sack, B. P., and Swanson, E. T. (2007), “Macroeconomic implications of changes in the term premium,” *Federal Reserve Bank of St Louis Review*, 89, 241–269.
- Rudebusch, G. D. and Wu, T. (2007), “Accounting for a shift in term structure behavior with no-arbitrage and macro-finance models,” *Journal of Money, Credit and Banking*, 39, 395–422.